

# Oxo- and Oxoperoxo-molybdenum(VI) Complexes with Aryl Hydroxamates: Synthesis, Structure, and Catalytic Uses in Highly Efficient, Selective, and Ecologically Benign Peroxidic Epoxidation of Olefins

Swarup K. Maiti,<sup>†</sup> K. M. Abdul Malik,<sup>‡</sup> Shalabh Gupta,<sup>§</sup> Santu Chakraborty,<sup>#</sup> Ashok K. Ganguli,<sup>§</sup> Alok K. Mukherjee,<sup>#</sup> and Ramgopal Bhattacharyya<sup>\*†</sup>

Department of Chemistry, Jadavpur University, Kolkata 700032, India, Department of Chemistry, Cardiff University, P.O. Box 912, Park Place, Cardiff CF10 3TB, U.K, Department of Chemistry, Indian Institute of Technology, Hauz Khas, New Delhi 110016, India, and Department of Physics, Jadavpur University, Kolkata 700032, India

Received April 28, 2006

A solution obtained by dissolving MoO<sub>3</sub> in H<sub>2</sub>O<sub>2</sub> reacts separately with secondary hydroxamic acids (viz., *N*-benzoyl *N*-phenyl hydroxamic acid (BPHAH), *N*-benzoyl *N*-ortho-, -meta-, -para-tolyl hydroxamic acids, (BOTHAH, BMTHAH, and BPTH AH, respectively), and *N*-cinnamoyl *N*-phenyl hydroxamic acid (CPHAH) affording [MoO(O<sub>2</sub>)(BPHA)<sub>2</sub>] (1), [MoO(O<sub>2</sub>)(BOTH A)<sub>2</sub>] (2), [MoO(O<sub>2</sub>)(BMTH A)<sub>2</sub>] (3), [MoO(O<sub>2</sub>)(BPTH A)<sub>2</sub>] (4), and [Mo(O)<sub>2</sub>(CPHA)<sub>2</sub>] (5), respectively. The O and O<sub>2</sub> are situated cis to each other in 2–4, but in each case, they are disordered and distributed over four sites. This disorder does not exist in the 6-coordinate cis dioxo complex 5, to which crude MoO(O<sub>2</sub>)(CPHA)<sub>2</sub> (5') was converted during recrystallization. An aqueous molybdate solution readily reacts with all those hydroxamic acids producing [Mo(O)<sub>2</sub>(hydroxamate)<sub>2</sub>] (6). While 2, 3, and 4 possess a very distorted pentagonal bipyramidal structure, 5 has a distorted octahedral geometry. In the solid state, as well as in solution, 5 exists as two apparently enantiomerically related molecules differing in the orientation of the pendant phenyl rings. To emphasize that the formation and structural uniqueness of 5 compared to 1–4 is caused by the influence of the cinnamoyl residue, one compound of the 6 series, namely, [Mo(O)<sub>2</sub>(BPHA)<sub>2</sub>] (6A), was structurally characterized to prove directly that the special stereochemical properties of 5 rely on the special electronic structure of CPHA<sup>−</sup> ligand. Complexes 1–5, as well as 6, show high potential and selectivity as catalysts in the epoxidation of olefins at room temperature in the presence of NaHCO<sub>3</sub> as a promoter and H<sub>2</sub>O<sub>2</sub> as a terminal oxidant. A comparative epoxidation study has been performed to determine the relative efficiency of the catalysts. To make the epoxidation method cost effective, a study to optimize the use of H<sub>2</sub>O<sub>2</sub> has also been performed. To obtain evidence in favor of our suggested mechanism to this homogeneous olefin → epoxide conversion, it was necessary to synthesize a peroxo-rich compound, namely, [Mo(O)<sub>2</sub>(BMTH A)]<sup>−</sup> (7), but the attempted synthesis culminated in the isolation of [Mo(O)<sub>2</sub>(C<sub>6</sub>H<sub>5</sub>COO)]<sup>−</sup> (8), obviously, via the hydrolysis of coordinated BMTH A.

## Introduction

Molybdenum and tungsten compounds in their higher oxidation states function as potential heterogeneous catalysts for organic oxidations.<sup>1</sup> We learned from biology<sup>2</sup> and

therefor evolved a model that shows<sup>3–5</sup> that a majority of the dioxomolybdenum(VI) complexes, generally possessing at least one S ligand, can use one of the oxygen atoms coming from one of the oxide ligands attached to molybdenum in the oxidation of organic, as well as inorganic, substrates and the two-step reduced oxomolybdenum(IV) moiety can be reoxidized to the dioxomolybdenum(VI) one via oxygen abstraction from a suitable substrate, thereby completing a two-substrate homogeneous catalytic cycle,<sup>6</sup>

\* To whom correspondence should be addressed. Phone: (+91) (+33) 2414-6193. Fax: (+91)(+33) 2414-6584. E-mail: aargibhatta@yahoo.com.

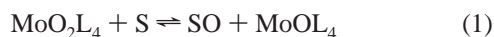
<sup>†</sup> Department of Chemistry, Jadavpur University,

<sup>‡</sup> Department of Chemistry, Cardiff University.

<sup>§</sup> Department of Chemistry, Indian Institute of Technology.

<sup>#</sup> Department of Physics, Jadavpur University.

as shown by simplified eqs 1 and 2. Mononuclear oxoperoxo-molybdenum(VI) frameworks are known to contain MoO(O<sub>2</sub>)<sub>2</sub> (i), MoO(O<sub>2</sub>)<sub>2</sub><sup>2+</sup> (ii), and Mo(O<sub>2</sub>)<sub>2</sub>(O<sub>2</sub>) (iii) motifs, but



the last one is seldom encountered. Epoxidation of olefins and arenes is a very outstanding transformation in organic synthesis since the epoxy compounds are widely used as is or for the manufacture of a wide variety of high-demand commodity chemicals such as polyurethanes, unsaturated resins, glycols, surfactants, and other products.<sup>7</sup> Transition metal complexes have a very dominant role as catalyst, which dramatically enhance the reaction yield, selectivity, and rate of epoxidation.<sup>8</sup> Also, H<sub>2</sub>O<sub>2</sub> is probably the best terminal oxidant after dioxygen with respect to environmental and economic considerations. Indeed, in certain circumstances, it is better than dioxygen because O<sub>2</sub>-organic mixtures can sometimes spontaneously ignite.<sup>9</sup> The effect of chelating ligands in the transition metal complexes is also important. [MoO(O<sub>2</sub>)<sub>2</sub>(C<sub>2</sub>O<sub>4</sub>)] oxidizes metal-bound thiolate species at rates approximately 10 times faster than does the complex<sup>10</sup> [MoO(O<sub>2</sub>)<sub>2</sub>(OH)(H<sub>2</sub>O)]<sup>-</sup>. Diperoxo complexes of d<sup>0</sup> transition metals, including Mo<sup>VI</sup> and W<sup>VI</sup>, are generally believed to be more reactive in this regard than the corresponding monoperoxo complexes, though examples exist where the reverse is also true.<sup>11,12</sup> A number of oxo-diperoxo-molybdenum(VI) complexes having the composition [MoO(O<sub>2</sub>)<sub>2</sub>(L-LH)(H<sub>2</sub>O)],<sup>13</sup> where L-LH stands for neutral bidentate α-amino acid ligands such as glycine, alanine, proline, valine, leucine, serine, and nicotinic acid *N*-oxide, among which a couple of complexes<sup>11,12</sup> were structurally characterized but

uptil now their catalytic functions remain unreported. Jacobson et al.<sup>14</sup> synthesized quite a few oxo-diperoxo-picolinato complexes of Mo and W and structurally characterized a couple of them, but they used them as catalysts in alcohol oxidation only.<sup>15</sup> Bartolini et al.<sup>16</sup> also studied the picolinate complexes again for alcohol oxidation, where in the case of one substrate, 20% epoxidation occurs along with 80% aldehyde formation.<sup>16</sup> The Mimoun-type peroxo complexes<sup>8c,17</sup> [MO(O<sub>2</sub>)<sub>2</sub>(L<sub>x</sub>)] (M = Mo, W; L = HMPT- (hexamethyl phosphoric triamide), DMF, R<sub>3</sub>PO (R = alkyl or aryl), DMSO, Py; x = 1, 2) have been extensively investigated as stoichiometric reagents for the epoxidation of olefins. However, only limited success could be achieved in the attempts to make those neutral molybdenum complexes catalytically active because of their poor ability<sup>18</sup> in hydrogen peroxide activation. However, slightly better results were obtained using tertiary butyl hydroperoxide (TBHP), but TBHP is more expensive and less environmentally friendly than H<sub>2</sub>O<sub>2</sub>. This was perhaps the reason for that the workers stopped using neutral peroxo complexes of Mo and also W (though it was much more active than Mo) in favor of the Venturello–Ishii strategy,<sup>18</sup> using heteropolyoxo metalates of W<sup>8b</sup> and, to a much lesser extent, of Mo. Heteropolyoxo-peroxo-tungstates such as (R<sub>4</sub>N)<sub>3</sub>{PO<sub>4</sub>[WO(O<sub>2</sub>)<sub>2</sub>]<sub>4</sub>} were isolated and characterized crystallographically by Venturello and co-workers.<sup>18a</sup> This type of W catalyst was found to use H<sub>2</sub>O<sub>2</sub> more efficiently than many other oxidation catalysts. A related Mo compound (viz., (NMe<sub>4</sub>)<sub>2</sub>[PhPO<sub>3</sub>{MoO(O<sub>2</sub>)<sub>2</sub>]<sub>2</sub>-(H<sub>2</sub>O)]) was also prepared, and its catalytic ability in epoxidation was examined:<sup>19</sup> it showed that it was much less efficient than the tungsten systems even in harsh reaction conditions. Even the W catalysts exhibited moderate turnovers and low selectivities, and so, the catalyst economy, which is a very important factor, was low. A good example for catalyst economy was provided by the isoelectronically related methyl trioxo-rhenium (MTO)<sup>20a,b</sup> and (PPh<sub>4</sub>)<sub>2</sub>[Re(NCS)<sub>6</sub>]<sup>20c</sup> catalysts with H<sub>2</sub>O<sub>2</sub> as a terminal oxidant. Despite the above quality, MTO is very expensive, and catalyst deactivation by the Re–C bond rupture during prolonged use made catalyst recycling a very difficult proposal. The thiocyanate complex is a bit less expensive and is easily synthesizable from KReO<sub>4</sub>; it is more efficient (TON and

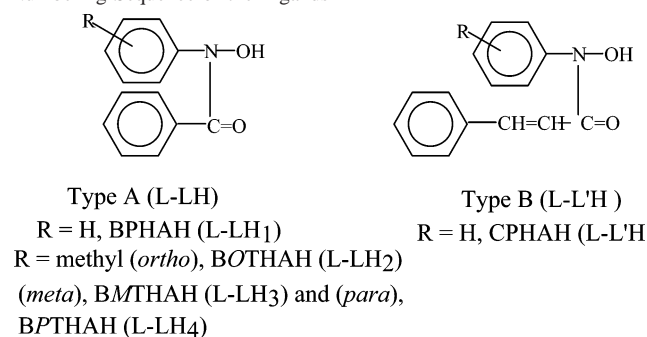
- (1) Davis, P.; Donald, R. T.; Harbard, N. H. *Catalyst Handbook*, 2nd ed.; Twigg, M. V., Ed.; Manson Publishing Ltd.: London, 1996.
- (2) (a) Bray, R. C. *The Enzymes*, 3rd ed.; Boyed, P. D., Ed.; Academic Press: New York, 1975; Vol. 12, Part B, Chapter 6. (b) Coughtan, M. P., Ed. *Molybdenum and Molybdenum Containing Enzymes*; Pergamon: New York, 1980. (c) Newton, W. E.; Otseeka, S., Eds. *Molybdenum Chemistry of Biological Significance*; Plenum: New York, 1980. (d) Cramer, S. P.; Wahl, R.; Rajagopalan, K. V. *J. Am. Chem. Soc.* **1981**, *103*, 7721–7727.
- (3) Xiao, Z.; Bruck, M. A.; Enemark, J. H.; Young, C. G.; Wedd, A. G. *Inorg. Chem.* **1996**, *35*, 7508–7515.
- (4) Eagle, A. A.; Harben, S. M.; Tiekink, E. R. T.; Young, C. G. *J. Am. Chem. Soc.* **1994**, *116*, 9749–9752.
- (5) Hille, R. *Chem. Rev.* **1996**, *96*, 2757–2816.
- (6) Bhattacharjee, S.; Bhattacharyya, R. *J. Chem. Soc., Dalton Trans.* **1992**, 1357–1364; **1993**, 1151–1158.
- (7) Weissmel, K.; Arpe, H. J. *Industrial Organic Chemistry*, 3rd ed.; VCH: Weinheim, Germany, 1997.
- (8) (a) Murphy, A.; Dubois, D.; Stack, T. D. P. *J. Am. Chem. Soc.* **2003**, *125*, 5250–5251. (b) Zuwei, X.; Ning, J.; Yu, S.; Kunlan, L. *Science* **2001**, *292*, 1139–1141. (c) Mimoun, H.; Sere de Roch, I.; Sajus, L. *Tetrahedron* **1970**, *26*, 37–50.
- (9) Lane, B. S.; Burgess, K. *Chem. Rev.* **2003**, *103*, 2457–2473.
- (10) Reynolds, M. S.; Morandi, S. J.; Raibiger, J. W.; McIcan, S. P.; Smith, S. P. E. *Inorg. Chem.* **1994**, *33*, 4977–4984.
- (11) (a) Bartolini, O.; Difuria, F.; Seremin, P.; Modena, G. *J. Mol. Catal.* **1980**, *7*, 59–74. (b) Thiel, W. R.; Eppinger, J. *Chem.—Eur. J.* **1997**, *3*, 696–705.
- (12) Abu-Omar, M. M.; Espenson, J. H. *J. Am. Chem. Soc.* **1995**, *117*, 272–280.
- (13) Djordjevic, C.; Vuletic, N.; Sinn, E. *Inorg. Chim. Acta* **1985**, *104*, L7–L9. (b) Djordjevic, C.; Puriar, B. C.; Vuletic, N.; Abelt, C. J.; Sheffield, S. J. *Inorg. Chem.* **1988**, *27*, 2926–2932.

- (14) Jacobson, S. E.; Tang, R.; Mares, F. *Inorg. Chem.* **1978**, *17*, 3055–3063.
- (15) Jacobson, S. E.; Muccigrosso, D. A.; Mares, F. *J. Org. Chem.* **1979**, *44*, 921–924.
- (16) Bartolini, O.; Camprestini, S.; Di Furia, F.; Modena, G.; Valle, G. *J. Org. Chem.* **1986**, *52*, 5467–5469.
- (17) (a) Mimoun, H.; Sere de Roch, I.; Sajus, L. *Bull. Soc. Chim. Fr.* **1969**, *5*, 1481–1492. (b) Winter, W.; Mark, C.; Schurig, V. *Inorg. Chem.* **1980**, *19*, 2045–2048.
- (18) (a) Venturello, C.; Alneri, E.; Ricci, M. *J. Org. Chem.* **1983**, *48*, 3831–3833. (b) Ishii, Y.; Yamayaki, K.; Yoshida, T.; Ura, T.; Ogawa, M. *J. Org. Chem.* **1987**, *52*, 1868–1870.
- (19) Csanyi, L. J.; Jaky, K. *J. Catal.* **1991**, *127*, 42–50. (b) Griffith, W. P.; Perkin, B. C.; White, A. J. P.; Williams, D. J. *J. Chem. Soc., Dalton Trans.* **1995**, 3131–3138.
- (20) Hermann, W. A.; Fischer, R. W.; Scherer, W.; Rauch, M. *Angew. Chem., Int. Ed. Engl.* **1993**, *32*, 1157–1160. (b) Hermann, W. A.; Ding, H.; Kratzer, R. M.; Kuhn, F. E.; Haider, J. J.; Fischer, R. W. *J. Organomet. Chem.* **1997**, *54*, 319–322. (c) Dinda, S.; Chowdhury, S. R.; Malik, K. M. A.; Bhattacharyya, R. *Tetrahedron Lett.* **2005**, *46*, 339–341.

TOF) than MTO, but the catalyst recovery in this case is also not very straightforward. This motivated the synthesis of new oxoperoxo-molybdenum and -tungsten complexes. An interesting report involving the isolation and structure determination of complexes of the type  $[\text{MoO}(\text{O}_2)_2(\text{L}_2)]$  (L = long chain trialkylamine oxide, -phosphane oxide, and -arsane oxide) appeared, and they were found to be catalytically active (with moderate efficiency) with  $\text{H}_2\text{O}_2$  as an oxidant.<sup>21</sup> Subsequently, it was found that even better epoxidation ability of the Mo and W oxoperoxo complexes could be achieved using the tri(*n*-dodecyl)-arsane oxide ligand under biphasic condition  $\text{CHCl}_3/30\% \text{H}_2\text{O}_2$  at  $60^\circ\text{C}$ .<sup>22</sup>

A few years ago we reported<sup>23</sup> the synthesis and structure of an oxo-peroxo complex involving motif ii, having the composition  $[\text{MoO}(\text{O}_2)(\text{QO})_2]$  (QO = 8-quinolinolate anion), which was the first molybdenum complex reported to function as a very efficient catalyst in the homogeneous oxidation of alkyl benzenes with  $\text{H}_2\text{O}_2$  as a terminal oxidant.<sup>23</sup> The above compound, as well as its diperoxo analogues  $[\text{MO}(\text{O}_2)_2 \cdot 2\text{QOH}]$  and  $[\text{MO}(\text{O}_2)_2(\text{QO})]^-$  (M = Mo, W), was also subsequently used by us<sup>24</sup> as an efficient catalyst in the oxidation of alcohols and sulfides.<sup>24,25</sup> In our continued interest in using oxo-peroxo-molybdenum, as well as -tungsten complexes, with  $\text{H}_2\text{O}_2$  as an oxidant, we reported a Mo-based catalyst (viz.,  $\text{PPh}_4[\text{MoO}(\text{O}_2)_2(\text{SaloxH})]$ )<sup>26</sup> and claimed an uncommon potentiality of the complex in olefin epoxidation. However, the said Mo complex was not very effective in epoxidizing higher olefins at room temperature. Our subsequent report was of a tungsten catalyst  $[\text{WO}(\text{O}_2)_2(\text{QO})]^-$  which took care of the higher alkenes, and it was found to possess a prolific efficiency<sup>27</sup> in olefin epoxidation. We now report that hydroxamic acids, which are known to function as bidentate O—O-donor<sup>28</sup> ligands,<sup>29</sup> form stable complexes with the oxo-diperoxo-molybdenum core and that such complexes, using secondary hydroxamic acids (L-LH as type A and L-L'H as type B ligands; see Scheme 1 where ligand abbreviation has also been shown), afford oxo-peroxo-molybdenum(VI) complexes. In this paper, we report the synthesis, structure (incidentally all the complexes, except for **8**, possess a butterflylike structure),<sup>30</sup> and catalytic potential of a number of such complexes in the epoxidation of olefins at room temperature using  $\text{NaHCO}_3$  as a cocatalyst and  $\text{H}_2\text{O}_2$  as a terminal oxidant. Interestingly, *in this case the Mo complexes are found to be more potent catalysts than*

**Scheme 1.** Structural Formulas, Abbreviative Notation, and Numbering Sequence of the Ligands



*the corresponding W complexes*,<sup>31</sup> which perhaps happened for the first time in Mo— $\text{H}_2\text{O}_2$ -catalysis research.

In this work, the parent ligand BPHAH (L-LH<sub>1</sub>) is derivatized to obtain four structurally analogous ligands (L-LH<sub>1</sub>–L-LH<sub>4</sub>, Scheme 1) by introducing methyl groups in the ortho, meta, or para positions, with respect to the carbon atom of the phenyl group attached to the N atom, to study the electronic versus steric control in the structure–reactivity relationship. The type B ligand, L-L'H, was chosen to create a situation in which the benzenoid  $\pi$  system is further coupled with a  $\pi$  residue (viz., the  $-\text{CH}=\text{CH}-\text{C}=\text{O}$  fragment of the cinnamoyl function of the CPHA ligand attached to the metal ion), and as a result, **5** exists as two apparently enantiomerically related molecules (both in the solid state and in the solution phase), differing from each other in the orientation of the pendant phenyl rings.

The herein isolated oxoperoxo complexes have the compositions  $[\text{MoO}(\text{O}_2)(\text{BPHA})_2]$  (**1**),  $[\text{MoO}(\text{O}_2)(\text{BOTHA})_2]$  (**2**),  $[\text{MoO}(\text{O}_2)(\text{BMTHA})_2]$  (**3**),  $[\text{MoO}(\text{O}_2)(\text{BPTH})_2]$  (**4**), and  $[\text{MoO}_2(\text{CPHA})_2]$  (**5**), as well as the labile complex  $[\text{MoO}(\text{O}_2)(\text{CPHA})_2]$  (**5'**). A plausible explanation for the conversion of **5'** to **5** during the crystallization process, in contrast to **1–4**, which all retain their identity under the above process, has been offered in the Discussion section. While writing this manuscript, we discovered that synthesis and structure of **1** was reported,<sup>32</sup> but its catalytic activity was not.<sup>33</sup> Hence,

- (21) Diekmann, M. H.; Pope, M. T. *Chem. Rev.* **1994**, *94*, 569–584.  
 (22) Jost, R.; Wahl, G.; Kleinheuz, D.; Sundermeyer, J. In *Peroxide Chemistry: Mechanistic and Preparative Aspects of Oxygen Transfer*; Adam, W., Ed.; Wiley-VCH: Weinheim, Germany, 2000; p 354–355.  
 (23) Bandyopadhyay, R.; Biswas, S.; Guha, S.; Mukherjee, A. K.; Bhattacharyya, R. *Chem. Commun.* **1999**, 1627–1628.  
 (24) Maiti, S. K.; Malik, K. M. A.; Bhattacharyya, R. *Inorg. Chem. Commun.* **2004**, *7*, 823–828.  
 (25) Maiti, S. K.; Bannerjee, S.; Mukherjee, A. K.; Malik, K. M. A.; Bhattacharyya, R. *New J. Chem.* **2005**, *29*, 554–563.  
 (26) Gharah, N.; Chakraborty, S.; Mukherjee, A. K.; Bhattacharyya, R. *Chem. Commun.* **2004**, 2630–2632.  
 (27) Maiti, S. K.; Dinda, S.; Gharah, N.; Bhattacharyya, R. *New J. Chem.* **2006**, *30*, 479–489.  
 (28) Si, T. K.; Chowdhury, K.; Mukherjee, M.; Bera, D. C.; Bhattacharyya, R. *J. Mol. Catal. A: Chem.* **2004**, *219*, 241–247. (b) Pecoraro, V. L. *Inorg. Chim. Acta* **1989**, *155*, 171–173.

- (29) A very limited number of synthetic works with type A ligands appeared in the literature, and no such work appeared with type B ligands. Reported work with type A ligands includes  $\text{Co}^{\text{II}}$ ,  $\text{Ni}^{\text{II}}$  (Mehrotra, R. C. In *Comprehensive Coordination Chemistry*; Wilkinson, G. S., Gillard, R. D., McCleverty, J. A., Eds.; Pergamon Press: New York, 1987; Vol. 2 and references therein),  $\text{Cr}^{\text{III}}$  (Weizman, H.; Libman, J.; Shanzer, A. *J. Am. Chem. Soc.* **1998**, *120*, 2188–2189), a few complexes of  $\text{Mn}^{\text{III}}$  and  $\text{Mn}^{\text{IV}}$  from this laboratory (Mukhopadhyay, R.; Chatterjee, A. B.; Bhattacharyya, R. *Polyhedron* **1992**, *11*, 1353–1358; Sahana, S.; Jana, T. K.; Bhattacharyya, R. *C. R. Chimie* **2005**, *8*, 1109–1121), and a dixouranium(VI) complex (Chakraborty, S.; Dinda, S.; Bhattacharyya, R.; Mukherjee, A. K. *Z. Kristallogr.* **2006**, *221*, 606–611). The hydroxamic acids are also well-known for their siderophoric roles and many other biologically important activities. They have also been used in chemical analysis (Majumdar, A. K. *N-Benzoylphenylhydroxylamine and its Analogues*; Belcher, R., Frieser, A., Eds.; Pergamon Press: Braunschweig, Germany, 1971 and references therein).  
 (30) Stone, F. G. A. *Pure Appl. Chem.* **1986**, *58*, 529–536. (b) Celenligil-Cetin, R.; Staples, R. J.; Staropoulos, P. *Inorg. Chem.* **2000**, *39*, 5838–5846. (c) Figueroa, J. S.; Cummins, C. C. *J. Am. Chem. Soc.* **2003**, *125*, 4020–4021.  
 (31) Maiti, S. K.; Dinda, S.; Bhattacharyya, R. Unpublished work.  
 (32) Tomioka, H.; Takai, K.; Oshima, K.; Nozaki, H. *Tetrahedron Lett.* **1980**, *21*, 4843–4846.

we include **1** in our work to compare its catalytic potential with that of **2–4**. Strikingly, not a single  $[\text{MoO}_2(\text{hydroxamate})_2]$  (**6**) was structurally characterized until now. For this reason, we had to isolate **6** with all the ligands used in oxoperoxo cases, and the structural characterization of  $[\text{MoO}_2(\text{BPHA})_2]$  (**6A**) indicates that it exists as a single molecule proving therefore that the enantiomerically related molecules in  $[\text{MoO}_2(\text{CPHA})_2]$  is a structurally unique case, resulting from the special type of electronic structure of CPHA compared to other hydroxamic acids. The catalytic potential of **6** using  $\text{NaHCO}_3$  as a cocatalyst and  $\text{H}_2\text{O}_2$  as an oxidant was also studied, and a probable mechanism of catalytic oxidation is reported. To obtain experimental evidence in favor of the suggested mechanism for catalytic substrate oxidation by **1–4**, a peroxo-rich oxomolybdenum complex  $[\text{MoO}(\text{O}_2)_2(\text{BMTHA})]^-$  (**7**) (as a representative case) was planned to be synthesized and characterized, but X-ray crystallography indicated that the synthesis resulted in the isolation of  $[\text{MoO}(\text{O}_2)_2(\text{C}_6\text{H}_5\text{—COO})]^-$  as  $\text{PPh}_4$  salt (**8**). Notably **8** could not be synthesized by sodium benzoate or benzoic acid in place of the BPHAH ligand.

The speciality of the present series of complexes lies in the selectivity and very high order of catalytic efficiency in the epoxidation of olefins at room temperature with high TOF ( $\text{TON h}^{-1}$ ). Our reported molybdenum-catalyzed epoxidation work<sup>26</sup> has, so far, an excellent efficiency, but we are now delighted to report that our present method using the described Mo hydroxamate complexes as catalysts show much higher efficiency in the epoxidation of more-reactive, less-reactive, and functionalized alkenes alike. Incidentally, the efficiency is even higher than that observed by Sharpless and co-workers<sup>34</sup> using  $\text{CH}_3\text{ReO}_3$  catalyst, amine additive like pyridine, 3-cyanopyridine, or pyrazole and  $\text{H}_2\text{O}_2$  as the terminal oxidant.

## Experimental Section

**Physical Measurements.** IR spectra were recorded as KBr pellets on a Perkin-Elmer 597 IR spectrophotometer ( $4000\text{--}200\text{ cm}^{-1}$ ), and the electronic spectra were recorded on a Hitachi U-3410 UV/VIS–NIR spectrophotometer.  $^1\text{H}$  and  $^{13}\text{C}$  NMR spectra were measured in  $\text{CDCl}_3$  on a Bruker AM 360 (300 MHz) FT NMR spectrometer using TMS as an internal standard. A Systronics (India) model 335 digital conductivity bridge with a bottle-type cell was used to determine the molar conductance values of the isolated complexes at  $25\text{ }^\circ\text{C}$  using a thermostatic arrangement. A SUNVIC (U.K.) apparatus was used to measure the melting points of the organic substrates, as well as those of their oxidized products. The magnetic susceptibilities were obtained by the Gouy method using  $\text{Hg}[\text{Co}(\text{NCS})_4]$  as a standard. Elemental analyses were performed with the help of a Perkin-Elmer 240C elemental analyzer, and molybdenum was estimated gravimetrically as its 8-quinolinolate.<sup>35</sup> HPTLC tests were performed in a CAMAG HPTLC system (Switzerland). GLC measurements were done in an Agilent model 6890 N gas chromatograph using an HP-1 and INNOWAX capillary column in FID mode with dinitrogen as carrier gas.

(33) However, virtually stoichiometric oxidation of olefinic alcohols to the corresponding epoxides and primary and secondary alcohols to corresponding carbonyl compounds was described there using expensive *tert*-butyl hydroperoxide as oxidant.

(34) Adolfsson, H.; Converso, A.; Sharpless, K. B. *Tetrahedron Lett.* **1999**, *40*, 3991–3994.

**Materials.** The compounds  $\text{MoO}_3\cdot 2\text{H}_2\text{O}$ , dinitrophenyl hydrazine, and zinc dust were of an extra-pure variety and were obtained from Loba Chemie (India). Hydrogen peroxide (30%), hydrochloric acid, ammonium chloride, sodium bicarbonate, acetonitrile, dichloromethane, light petroleum (40–60), diethyl ether, and acetone were of analytical grade and were obtained from E. Merck (India). Cyclopentene, cyclohexene, cyclooctene, norbornene, 1-buten-3-ol, 4-penten-1-ol, *cis*-2-penten-1-ol, 1-hexene, 2-hexen-1-ol, 1-heptene, 1-octene, 1-octene-2-ol, 1-decene, *trans*-5-decene, and 1-dodecene were the products of Sigma Aldrich Chemie GmbH, Germany, and were used directly. Styrene, cinnamyl alcohol, and allyl alcohol were obtained from E. Merck (Germany). All the epoxides of the corresponding olefins were the products of Aldrich, U.S.A. Nitrobenzene and *o*-, *m*-, and *p*-nitrotoluenes of laboratory reagent grade were obtained from B. D. H. (India). Benzoyl chloride and thionyl chloride of synthetic reagent grade were obtained from Ranbaxy (India). Ethanol (95%) was obtained from Bengal Chemical and Pharmaceutical works (Calcutta, India), and it was lime-distilled before use. IOLAR II grade dioxygen, dihydrogen, zero air, and dinitrogen gas used for chromatographic analysis were obtained from Indian Refrigeration Stores (Calcutta, India). Triple-distilled (all glass) water was used whenever necessary. The hydroxamic acid ligand (viz., L-LH<sub>1</sub>–LLH<sub>4</sub> and L–L'H) ligands were prepared following the literature method<sup>29</sup> and characterized by elemental analysis, melting point, and IR data. All the solvents used for chromatographic analysis were either of HPLC, spectroscopic, or GR grade.

**Preparation of the Complexes.  $[\text{MoO}(\text{O}_2)(\text{BPHA})_2]$  (**1**).** The preparation method of **1**, which is substantially different from and more convenient with a higher yield than the earlier method,<sup>32</sup> is described as follows: Hydrated molybdenum trioxide,  $\text{MoO}_3\cdot 2\text{H}_2\text{O}$  (0.45 g, 2.5 mmol) was dissolved in a 30% w/v hydrogen peroxide solution (4 mL) by stirring at room temperature ( $25\text{ }^\circ\text{C}$ ). BPHAH (1.02 g, 5.0 mmol) was dissolved in a minimum volume of ethanol (~5 mL), and the resulting solution was added to the previous solution, with stirring (5min) when a yellow solid separated. The solid was filtered off, washed with water, ethanol, and diethyl ether, and dried in vacuo. The compound was crystallized as pale yellow rectangle from a dichloromethane/*n*-hexane (1:1) solvent mixture. Yield 1.14 g (2.1 mmol, 82.8%). Anal. Calcd for  $\text{C}_{26}\text{H}_{20}\text{N}_2\text{O}_7\text{Mo}$ : C, 54.92; H, 3.52; N, 4.92; Mo, 16.90. Found: C, 54.70; H, 3.54; N, 4.70; Mo, 16.72. The compound is soluble in acetone, acetonitrile, and dichloromethane, but it is insoluble in ether, benzene, and carbon tetrachloride. IR (KBr disk,  $\text{cm}^{-1}$ ):<sup>36,37</sup> 1600 (m), 1550 (s,  $\nu(\text{C}=\text{O})$ ), 1500 (m), 1460 (m), 1430 (m,  $\nu(\text{C}-\text{N})$ ), 1300 (vw), 1160 (w), 1080 (vw), 1040 (w), 1020 (m), 960 (s,  $\nu(\text{Mo}=\text{O})$ ), 910 (m,  $\nu(\text{O}-\text{O})$ ), 780 (m), 720 (w), 700 (s), 690 (w), 640 (w), 590 (w), 560 (m), 500 (w), 450 (w), 310 (w). UV–vis ( $\lambda_{\text{max}}$  (nm),  $\epsilon$  ( $\text{M}^{-1}\text{ cm}^{-1}$ )): 235 (sh), 270 (sh), 360 (1460).<sup>38</sup>

**$[\text{MoO}(\text{O}_2)(\text{BOTH A})_2]$  (**2**),  $[\text{MoO}(\text{O}_2)(\text{BMTH A})_2]$  (**3**), and  $[\text{MoO}(\text{O}_2)(\text{BP TH A})_2]$  (**4**).** These compounds were prepared and crystallized by following the same method as described under **1** using the corresponding hydroxamic acid ligands instead of BPHAH. Anal. Calcd for  $\text{C}_{28}\text{H}_{24}\text{N}_2\text{O}_7\text{Mo}$  (i.e., **2**, **3**, **4**): C, 56.37; H, 4.03; N, 4.70; Mo, 16.10. For **2**, found: C, 56.48; H, 4.14; N,

(35) Jeffery, G. H.; Bassett, J.; Mendham, J.; Denny, R. C., Eds. *Vogel's Text Book of Quantitative Chemical Analysis*, 5th ed.; Longman Scientific & Technical: Harlow, Essex, U.K., 1989.

(36) For authentication of the band assignment, see refs 23 and 29 (Mukhopadhyay et al.) in addition to 44 and 45.

(37) Rao, C. N. R.; Venkataraghavan, R. *Spectrochim. Acta* **1962**, *18*, 273. (b) Salinas, F.; Martinez-Vidal, J. L.; Gonzalez-Parra, J. *Proc.—Indian Acad. Sci., Chem. Sci.* **1985**, *95*, 265.

(38) Determined by Gaussian analysis.

4.74; Mo, 15.72. For **3**, found: C, 56.13; H, 4.08; N, 4.88; Mo, 15.62. For **4**, found: C, 56.44; H, 4.06; N, 4.74; Mo, 15.50. Solubilities for **2–4** are also similar to that of **1**. Yield (av): 83%. IR: for **2** 1605 (m), 1555 (s,  $\nu$  (C=O)), 1520 (m), 1460 (s), 1400 (vw, sh), 1315 (w), 1165 (w), 1150 (w), 1030 (m), 960 (s,  $\nu$ (Mo=O)), 910 (m,  $\nu$ (O–O)), 780 (s), 730 (m), 700 (s), 685 (m), 650 (m), 580 (w), 570 (m), 500 (w), 440 (w), 310 (w). UV–vis ( $\lambda_{\max}$  (nm) ( $\epsilon$  (M<sup>-1</sup> cm<sup>-1</sup>)): 225 (sh), 270 (14 805), 360 (570)<sup>36</sup>. <sup>1</sup>H NMR (CDCl<sub>3</sub>, TMS):  $\delta$  2.49 (s, 3H, –CH<sub>3</sub>{C14}),<sup>39</sup> 2.36 (s, 3H, –CH<sub>3</sub>–{C27}), 7.17–7.56 (m, 18H, aryl). <sup>13</sup>C{<sup>1</sup>H} NMR:  $\delta$  126.80, 127.20 (C14, C28), 127.40 (2C, C25, C11), 128.10 (2C, C26, C24), 128.40 (2C, C19, C5), 128.54 (2C, C10, C12), 128.90 (2C, C18, C20), 129.10 (2C, C4, C6), 129.23 (2C, C8, C22), 130.70 (C9/C23), 131.30, 131.60, 131.70, 131.77 (C7, C3, C21, C17), 132.60 (C23/C9), 136.30, 136.60 (C13, C27), 137.90 (C16), 138.60 (C2), 164.00, 164.40 (C1, C15). IR: for **3** 1620 (w), 1560 (s), 1540 (s), 1500 (s) (last three for  $\nu$ (C=O)), 1500 (sh), 1465 (s), 1455 (s), 1420 (sh, may be  $\nu$ (C–N)), 1290 (vw), 1320 (vw), 1310 (vw), 1200 (w), 1160 (m), 1100 (vw), 1080 (vw), 1060 (m), 1050 (m), 1000 (w), 980 (s,  $\nu$ (Mo=O)), 920 (m,  $\nu$ (O–O)),<sup>23</sup> 860 (w), 840 (m), 810 (s), 790 (m), 720 (m), 710 (sh), 700 (s), 680 (w), 670 (m), 650 (m), 600 (m), 580 (s), 570 (sh), 460 (w), 450 (m), 345 (w), 320 (w). UV–vis ( $\lambda_{\max}$  (nm) ( $\epsilon$  (M<sup>-1</sup> cm<sup>-1</sup>)): 225 (sh), 270 (13945), 360 (315). <sup>1</sup>H NMR:  $\delta$  2.35 (s, 3H, –CH<sub>3</sub>{C14}), 2.36 (s, 3H, –CH<sub>3</sub>{C28}), 7.00–7.56 (m, 18H, Ar). <sup>13</sup>C{<sup>1</sup>H} NMR:  $\delta$  123.52 (C14/C28), 123.80 (C28/C14), 126.90 (2C, C11, C25), 127.20 (2C, C9, C23), 128.00 (2C, C5, C19), 128.45 (2C, C10, C24), 129.00 (2C, C12, C26), 129.10 (2C, C18, C20), 129.39, 129.64 (C6, C4), 130.37, 131.00 (C13, C27), 132.45 (2C, C8, C22), 138.80, 139.20, 139.70, 139.96 (C3, C21, C7, C17), 163.69, 164.86 (C1, C5). IR: for **4** 1600 (w), 1590 (w), 1535 (s), 1500 (s){both the (s)  $\nu$ (C=O)}, 1450 (s), 1400 (sh, may be  $\nu$ (C–N)), 1280 (w), 1210 (vw), 1185 (w), 1150 (w), 1110 (w), 1085 (vw), 1030 (m), 1010 (m), 950 (s,  $\nu$ (Mo=O)), 930 (sh), 900 (m), 820 (m), 790 (w), 780 (m), 700 (s), 635 (m), 580 (sh), 560 (m), 500 (m), 445 (w), 390 (vw), 310 (w). UV–vis ( $\lambda_{\max}$  (nm) ( $\epsilon$  (M<sup>-1</sup> cm<sup>-1</sup>)): 225 (39 000), 270 (15 680), 360 (360).<sup>38</sup> <sup>13</sup>C{<sup>1</sup>H} NMR:  $\delta$  126.36, 126.62 (C14, C14'), 127.27 (2C, C11, C11'), 128.00 (2C, C10, C12), 128.47 (2C, C10', C12'), 128.70 (2C, C5, C5'), 129.44 (2C, C4, C6), 129.69 (2C, C4', C6'), 130.1 (2C, C9', C13'), 131.52, 132.37 (C13, C14), 136.40 (2C, {C3, C7}/{C3', C7'}), 137.57 (2C, {C3', C7'}/{C3, C7}), 139.89, 140.70 (C2, C2'), 163.66, 164.89 (C1, C1').

[Mo(O)<sub>2</sub>(CPHA)<sub>2</sub>] (**5'**). An H<sub>2</sub>O<sub>2</sub> solution of MoO<sub>3</sub>·2H<sub>2</sub>O of identical concentration as that in **1–4** was obtained in a manner similar to that described. *N*-cinnamoyl *N*-benzoyl hydroxamic acid (a type B ligand, see the Scheme; 1.09 g, 5.0 mmol) dissolved in minimum volume of ethanol (~5 mL) was added to the above solution, and the resulting solution was stirred for 4 min until a light greenish yellow solid separated. The precipitate was filtered off, washed with water, ethanol, and diethyl ether, and finally, dried in vacuo. Anal. Calcd for C<sub>30</sub>H<sub>24</sub>N<sub>2</sub>O<sub>7</sub>Mo: C, 58.06; H, 3.87; N, 4.51; Mo, 15.48. Found: C, 58.18; H, 3.94; N, 4.58; Mo, 15.24. Yield: 1.24 g (80%). Solubility is almost identical to that of **1–4**. IR: 1700 (s), 1650 (w), 1640 (w), 1615 (s,  $\nu$ (C=O)), 1545 (m), 1535 (s), 1470 (broad), 1280 (w), 1220 (w), 1060 (m), 1035 (m), 950 (s,  $\nu$ (Mo=O)), 910 (m,  $\nu$ (O–O)), 900 (w), 800 (m), 780 (sh), 760 (s), 700 (s), 640 (m), 620 (w), 600 (w), 560 (m), 545 (s), 405 (w), 390 (w). UV–vis ( $\lambda_{\max}$  (nm) ( $\epsilon$  (M<sup>-1</sup> cm<sup>-1</sup>)): 292 (39145), 330 (1495).<sup>38</sup> <sup>1</sup>H NMR:  $\delta$  6.38 (d, 1H, Ph-CH=CH–), 6.55 (d, 1H, Ph-CH=CH–), 7.25–7.75 (m, 21H, 20 for Ph and 1H for Ph-CH=CH–), 7.99 (d, 1H, Ph-CH=CH–). <sup>13</sup>C{<sup>1</sup>H} NMR:  $\delta$  for

molecule 1 123.52 (C14/C28), 123.80 (C28/C14), 126.90 (2C, C11, C25), 127.20 (2C, C9, C23), 128.00 (2C, C5, C19), 128.45 (2C, C10, C24), 129.00 (2C, C12, C26), 129.10 (2C, C18, C20), 129.39, 129.64 (C6,C4), 130.37, 131.00 (C13, C27), 132.45 (2C, C8, C22), 138.80, 139.70, 139.20, 139.96 (C3, C7, C21, C17), 163.69 (2C, C1, C5); for molecule 2 126.36, 126.62 (C14, C14'), 127.27 (2C, C11, C11'), 128.00 (2C, C10, C12), 128.47 (2C, C10', C12'), 128.70 (2C, C5, C5'), 129.44 (2C, C4, C6), 129.69 (2C, C4', C5'), 130.13 (2C, C9', C13'), 131.52, 132.37 (C13, C14), 136.40 (2C, {C3, C7}/{C3', C7'}), 137.57 (2C, {C3', C7'}/{C3, C7}), 139.89, 140.70 (C2, C2'), 163.66, 164.89 (C1, C1'). In complex **5**, 14 extra <sup>13</sup>C signals (for aromatic carbons) are obtained compared to the others (**2–4**), and so, they are logistically apportioned between molecule 1 and molecule 2.

[Mo(O)<sub>2</sub>(CPHA)<sub>2</sub>] (**5**). **5'** (1.24 g), obtained as above, was crystallized from a dichloromethane/hexane (1:1) mixture, and the light greenish-yellow plates deposited were filtered off and washed with light petroleum (40–60). Anal. Calcd for C<sub>30</sub>H<sub>24</sub>N<sub>2</sub>O<sub>6</sub>Mo: C, 59.59; H, 3.97; N, 4.64; Mo, 15.89. Found: C, 59.72; H, 4.08; N, 4.69; Mo, 15.64. Solubility is almost identical with those of **1–4**. IR: 1640 (s), 1610 (w), 1600 (w), 1535 (s,  $\nu$ (C=O)), 1540 (m), 1510 (s), 1485 (m), 1200 (w), 1040 (m, broad), 1030 (m), 1010 (w), 990 (w), 950 (s), 910 (s) (both the (s)  $\nu$ (Mo=O) from the *cis*-MoO<sub>2</sub><sup>2+</sup> moiety), 800 (m), 780 (sh), 760 (s), 690 (s), 680 (m), 625 (w), 610 (w), 580 (m), 560 (sh), 550 (m), 625 (w), 605 (sh), 580 (m), 550 (m), 505 (w), 475 (w), 400 (w), 360 (w), 330 (w), 300 (w). UV–vis ( $\lambda_{\max}$  (nm) ( $\epsilon$  (M<sup>-1</sup> cm<sup>-1</sup>)): 292 (38 540), 330 (sh).

**Synthesis of [Mo(O)<sub>2</sub>(BPHA)<sub>2</sub>](6A), [Mo(O)<sub>2</sub>(BOTHA)<sub>2</sub>](6B), [Mo(O)<sub>2</sub>(BMTHA)<sub>2</sub>](6C), [Mo(O)<sub>2</sub>(BPTHA)<sub>2</sub>](6D), Generalized as [MoO<sub>2</sub>(hydroxamate)<sub>2</sub>](6). General Method.** Hydrated sodium molybdate, Na<sub>2</sub>MoO<sub>4</sub>·2H<sub>2</sub>O (0.625 g, 2.5 mmol), was dissolved in a minimum volume of water (5 mL), and an ethanolic solution of the respective hydroxamic acid (5 mmol) was added dropwise to the aqueous solution with stirring until a light yellow solid separated out after the addition of 2 drops of hydrochloric acid (6 M). The solid was filtered off, washed thoroughly with distilled water, ethanol, and diethyl ether, and finally, dried in vacuo. All the compounds were crystallized from a dichloromethane/*n*-hexane solvent mixture. The yield was 86% for **6A**, 85% (av) for **6B** and **6C**, and 80% for **6D**. Anal. Calcd for C<sub>26</sub>H<sub>20</sub>N<sub>2</sub>O<sub>6</sub>Mo: C, 56.52; H, 3.62; N, 5.07; Mo, 17.39. For **6A**, found: C, 56.28; H, 3.54; N, 4.92; Mo, 17.16. Anal. Calcd for C<sub>28</sub>H<sub>24</sub>N<sub>2</sub>O<sub>6</sub>Mo: C, 57.93; H, 4.13; N, 4.82; Mo, 16.55. For **6B**, found: C, 58.06; H, 4.42; Mo, 4.85; Mo, 16.20. For **6C**, found: C, 57.82; H, 4.18; N, 4.24; Mo, 16.12. For **6D**, found: C, 57.96; H, 4.16; N, 4.89; Mo, 16.05. IR: for **6A** 1600 (m), 1530 (s, broad,  $\nu$ (C=O)), 1470 (s), 1450 (s), 1300 (w), 1185 (m), 1180 (m), 1080 (m), 1040 (s), 1020 (s), 1000 (m), 940 (s,  $\nu$ (Mo=O)), 905 (s,  $\nu$ (Mo=O)), 790 (s), 720 (s), 700 (s), 680 (s), 630 (s), 610 (m), 560 (s), 500 (m), 480 (w), 450 (m), 405 (w), 375 (vw), 315 (s). UV–vis ( $\lambda_{\max}$  (nm) ( $\epsilon$  (M<sup>-1</sup> cm<sup>-1</sup>)): 301 (11 440), 356 (sh). IR: for **6B** 1610 (w), 1590 (m), 1540 (s,  $\nu$ (C=O)), 1500 (m), 1450 (m), 1440 (m), 1380 (w), 1290 (w), 1160 (w), 1140 (w), 1120 (w), 1070 (w), 1040 (w), 1010 (m), 950 (s,  $\nu$ (Mo=O)), 910 (s,  $\nu$ (Mo=O)), 800 (w), 780 (m), 770 (m), 700 (s), 660 (m), 640 (w), 620 (w), 590 (w), 570 (m), 560 (w), 450 (w), 310 (vw). UV–vis ( $\lambda_{\max}$  (nm) ( $\epsilon$  (M<sup>-1</sup> cm<sup>-1</sup>)): 225 (sh), 268 (12 990), 350 (sh). IR: for **6C** 1620 (w), 1600 (w), 1530 (s,  $\nu$ (C=O)), 1510 (w), 1460 (m), 1450 (w), 1200 (w), 1150 (w), 1060 (w), 1010 (w), 960 (m), 955 (m), 940 (s,  $\nu$ (Mo=O)), 910 (v,  $\nu$ (Mo=O)), 840 (m), 800 (m), 780 (m), 710 (m), 700 (s), 660 (w), 640 (w), 560 (m), 450 (w), 440 (w), 300 (vw). UV–vis ( $\lambda_{\max}$  (nm) ( $\epsilon$  (M<sup>-1</sup> cm<sup>-1</sup>)): 226 (sh), 267 (13 245), 352 (sh). IR: for **6D**

(39) Numbers after C in all the cases indicate those that appear in the respective ORTEP diagrams.

1600 (w), 1580 (w), 1540 (s,  $\nu(\text{C}=\text{O})$ ), 1520 (m), 1450 (m), 1210 (w), 1180 (w), 1150 (w), 1100 (w), 1070 (vw), 1030 (m), 1010 (m), 960 (m), 940 (s,  $\nu(\text{Mo}=\text{O})$ ), 910 (s,  $\nu(\text{Mo}=\text{O})$ ), 820 (m), 800 (w), 780 (m), 720 (w), 710 (m), 700 (m), 645 (w), 640 (w), 560 (m), 510 (w), 460 (vw), 440 (w), 310 (vw). UV-vis ( $\lambda_{\text{max}}$  (nm) ( $\epsilon$  ( $\text{M}^{-1} \text{cm}^{-1}$ )): 226 (sh), 268 (13 840), 352 (sh).

**[PPh<sub>4</sub>][MoO(O<sub>2</sub>)<sub>2</sub>(C<sub>6</sub>H<sub>5</sub>-COO)] (8).** [MoO(O<sub>2</sub>)(BMTHA)<sub>2</sub>] (2.50 mmol, 1.42 g) was dissolved in a minimum volume of acetonitrile (15 mL) in a round-bottomed flask and was refluxed for 1 h after the addition of an excess of H<sub>2</sub>O<sub>2</sub> (30% w/v, 20 mL) until a uniform clear solution was obtained. Acetonitrile was then distilled out, and an aqueous solution (10 mL) of PPh<sub>4</sub>Cl (2.50 mmol, 0.86 g) was added dropwise to the remaining aqueous solution; the mixture was stirred constantly for 30 min until a reddish solid separated. The solid was filtered off, washed thoroughly with water, ethanol, and diethyl ether, and then dried in vacuo. The substance was found to be soluble in acetonitrile, acetone, dichloromethane, and chloroform but insoluble in diethyl ether and benzene. The compound was crystallized from a dichloromethane/hexane (1:1) solvent mixture. Yield: 0.98 g (62%). Anal. Calcd for C<sub>31</sub>H<sub>25</sub>O<sub>7</sub>MoP: C, 58.49; H, 3.93; Mo, 15.09. Found: C, 58.56; H, 4.04; Mo, 14.94. IR: 1610 (m), 1580 (s,  $\nu(\text{C}=\text{O})_{\text{sym}}$ ), 1500 (s,  $\nu(\text{C}=\text{O})_{\text{asym}}$ ), 1450 (s), 1380 (s), 1110 (s), 1030 (vw), 1000 (w), 970 (s,  $\nu(\text{Mo}=\text{O})$ ), 870 (s,  $\nu(\text{O}-\text{O})$ ), 760 (m), 720 (s), 695 (s), 655 (w), 580 (m), 530 (s), 460 (w), 310 (vw). UV-vis ( $\lambda_{\text{max}}$  (nm) ( $\epsilon$  ( $\text{M}^{-1} \text{cm}^{-1}$ )): 275 (6130), 268 (6810).

**X-ray Crystallography.** X-ray quality crystals of [MoO(O<sub>2</sub>)-(BOTH<sub>A</sub>)<sub>2</sub>] (**2**), [MoO(O<sub>2</sub>)(BMTHA)<sub>2</sub>] (**3**), [MoO(O<sub>2</sub>)(BPTH<sub>A</sub>)<sub>2</sub>] (**4**), [Mo(O<sub>2</sub>)(CPHA)<sub>2</sub>] (**5**), [Mo(O<sub>2</sub>)(BPHA)<sub>2</sub>] (**6A**), and [PPh<sub>4</sub>]-[MoO(O<sub>2</sub>)<sub>2</sub>(C<sub>6</sub>H<sub>5</sub>-COO)] (**8**) were obtained by adjusting the proportion of dichloromethane and pentane (some finer adjustment in the 1:1 mainframe procedure) in the mixed solvent so that crystallization started after 24 h. Intensity data for **2–5** were recorded using an Enraf Nonius CAD4 diffractometer ( $\omega$  scan) and monochromated Mo K $\alpha$  radiation ( $\lambda = 0.71073 \text{ \AA}$ ). The unit cell parameters for these complexes were determined by least-squares refinement of the setting angles for 25 reflections within  $17 \leq \theta \leq 18^\circ$ . The intensity data for **6A** and **8** were recorded using a Bruker SMART CCD area detector diffractometer using Mo K $\alpha$  radiation ( $\lambda = 0.71073 \text{ \AA}$ ). The unit cell parameters for these two compounds were refined on the basis of all the observed reflections in the whole data set. The data were corrected for Lorentz and polarization factors and also for absorption effects using DIFABS<sup>40a</sup> for **2–5** and SORTAV<sup>40b</sup> for **6A** and **8**. The structures were solved by direct methods (SHELXS-96)<sup>41</sup> and refined by full-matrix least-squares on  $F^2$  using all unique data (SHELXL-97).<sup>42</sup> The O and O<sub>2</sub> groups in **2**, **3**, and **4** were disordered and distributed over four sites. For **2**, each of the four positions, O(1)–O(4), was refined with occupancy 0.75; for **3**, the O(1) and O(2) positions were fully occupied, and O(3) and O(4) were both half occupied. For **4**, which contains a crystallographic 2-fold axis passing through the Mo atom, the two unique oxygen positions, O(1) and O(2), were assigned occupancies of 1.0 and 0.5, respectively. The models thus adopted for these compounds were consistent with stereochemistry and considered satisfactory, although the temperature factors for the half-occupied O(3) and O(4) sites in **3** were relatively higher than expected. The reasons for this anomaly are not immediately obvious. Compound **5** was free from disorder. It was solved and successfully

refined in the noncentrosymmetric space group  $P2_1$  with two molecules in the asymmetric unit. The two molecules appeared to be related by a pseudomirror plane, but attempts to solve the structure in the centrosymmetric space group  $P2_1/m$  were not successful. The Flack parameter<sup>43</sup> in SHELXL-97 had a final value of 0.00(5) indicating that the absolute structure had been determined correctly. It was concluded that the apparently mirror-related two molecules are two enantiomers of the central octahedron; each with correct configuration, but they differ in the orientation of the pendant phenyl rings. The crystal structures of **6A** and **8** are free from disorder. In **6A**, the Mo atom lies on a two-fold axis with half of the complex composing the asymmetric unit. In all structures, the non-hydrogen atoms were refined anisotropically, and the hydrogen atoms were included in calculated positions (riding model). The crystal data and refinement results are given in Table 1.

**Experimental Procedure of Epoxidation and Isolation of Products.** The experimental procedure for the epoxidation reaction involving a wide variety of olefinic substrates is described as follows: An acetonitrile (10 cm<sup>3</sup>) solution containing a given substrate ( $\sim 10$ – $15$  mmol), NaHCO<sub>3</sub> (2.5–3.75 mmol), a molybdenum catalyst (0.01–0.001 mmol), and 30% H<sub>2</sub>O<sub>2</sub> (30–40 mmol) in a flat bottom two-neck reaction flask with one neck fitted with a reflux condenser (to check evaporation) and the other neck closed with a septum was stirred at room temperature (25 °C) for a definite period as presented in the Table 3. When required, an aliquot of the reaction solution was withdrawn from the flask and H<sub>2</sub>O<sub>2</sub> was added to the contents of the flask with the help of a syringe through the septum. The withdrawn 0.5 cm<sup>3</sup> solution was subjected to multiple ether extractions, and the extract was concentrated to 0.5 cm<sup>3</sup> from which 1  $\mu\text{L}$  of solution was withdrawn with the help of a gas syringe and injected into the GC port. The retention times of the peaks were compared with those of commercial standards, and for the GC yield calculation, nitrobenzene was used as an internal standard. In a few cases, especially for olefinic alcohols, the identities of the products were confirmed by GC-MS analysis. The isolated yield in a few cases (Table 3) is obtained by multiple ether extractions of the reaction solution after the reaction is over, followed by evaporation of the ether and acetonitrile by distillation at a mildly reduced pressure (using water aspirator). The products were kept over P<sub>2</sub>O<sub>5</sub> in a desiccator and weighed (when the GC yield was 98–99%) in a microbalance, and then the identity of the products was confirmed by IR and NMR. For lower yield (%), the liquid (for solid epoxides obtained from liquid olefins, the former are simply dried and weighed) products were subjected to preparative TLC, and the highly intense spot was cut out and plunged into CH<sub>2</sub>Cl<sub>2</sub>, which serves as an eluant; then the resulting solution was dried over MgSO<sub>4</sub>, filtered through a short silica gel pad, and finally, evaporated to yield only the epoxide as residue by the distillation method as described above. The residue was then kept over P<sub>2</sub>O<sub>5</sub> for 15 min and weighed.

**Recovery of Catalyst.** The residue left after distillation of the ether and acetonitrile at mildly reduced pressure was thoroughly shaken with diethyl ether repeatedly until each of the substrates and the products were almost quantitatively extracted in the ether solvent and the yellow solid residue left was the catalyst as verified by IR spectroscopy.

## Results and Discussion

**A. Synthetic Aspects.** All the complexes (viz, **1–4** and **5'**) can be easily synthesized with a high yield by first

(40) Walker, N. P. C.; Stuart, D. *Acta Crystallogr.* **1983**, *A39*, 158–166.

(b) Blessing, R. H. *Acta Crystallogr.* **1990**, *A46*, 467–473.

(41) Sheldrick, G. M. *Acta Crystallogr.* **1990**, *A46*, 467–473.

(42) Sheldrick, G. M. *SHELXL, Program for Crystal Structure Refinement*; University of Göttingen: Göttingen, Germany, 1997.

(43) Flack, H. D. *Acta Crystallogr.* **1983**, *A39*, 876–881.

**Table 1.** Crystallographic Data<sup>a</sup> and Refinement Results for [MoO(O<sub>2</sub>)(BOTHA)<sub>2</sub>] (**2**), [MoO(O<sub>2</sub>)(BMTHA)<sub>2</sub>] (**3**), [MoO(O<sub>2</sub>)(BPTHA)<sub>2</sub>] (**4**), [MoO(O<sub>2</sub>)(CPHA)<sub>2</sub>] (**5**), [Mo(O<sub>2</sub>)(BPHA)<sub>2</sub>] (**6A**), and PPh<sub>4</sub>[MoO(O<sub>2</sub>)<sub>2</sub>(PhCOO)]<sup>-</sup> (**8**)

	<b>2</b>	<b>3</b>	<b>4</b>	<b>5</b>	<b>6A</b>	<b>8</b>
chemical formula	C <sub>28</sub> H <sub>24</sub> MoN <sub>2</sub> O <sub>7</sub>	C <sub>28</sub> H <sub>24</sub> MoN <sub>2</sub> O <sub>7</sub>	C <sub>28</sub> H <sub>24</sub> MoN <sub>2</sub> O <sub>7</sub>	C <sub>30</sub> H <sub>24</sub> MoN <sub>2</sub> O <sub>6</sub>	C <sub>26</sub> H <sub>20</sub> MoN <sub>2</sub> O <sub>6</sub>	C <sub>31</sub> H <sub>25</sub> MoO <sub>7</sub> P
fw (g/mol)	596.43	596.43	596.43	604.45	552.38	636.42
cryst syst	monoclinic	monoclinic	monoclinic	monoclinic	monoclinic	triclinic
space group	<i>P</i> 2 <sub>1</sub> / <i>n</i>	<i>P</i> 2 <sub>1</sub> / <i>n</i>	<i>C</i> 2/ <i>c</i>	<i>P</i> 2 <sub>1</sub>	<i>C</i> 2/ <i>c</i>	<i>P</i> 1
<i>a</i> (Å)	13.022(3)	10.457(2)	13.054(2)	12.992(3)	12.459(1)	10.366(1)
<i>b</i> (Å)	15.074(3)	16.428(4)	14.717(3)	15.033(3)	15.221(1)	10.970(1)
<i>c</i> (Å)	13.912(4)	15.056(3)	15.073(2)	14.646(3)	13.723(1)	12.836(1)
α (deg)	90.00	90.00	90.00	90.00	90.00	99.81(1)
β (deg)	90.48(2)	98.36(2)	99.43(2)	109.43(2)	92.852(20)	103.92(1)
γ (deg)	90.00	90.00	90.00	90.00	90.00	96.46(1)
95.62(8)						
<i>V</i> (Å <sup>3</sup> )	2730.8(12)	2559.1(9)	2856.5(7)	2697.6(9)	2599.20(4)	1378.13(15)
<i>Z</i>	4	4	4	4	4	2
ρ <sub>calcd</sub> (Mg/m <sup>3</sup> )	1.451	1.548	1.387	1.488	1.412	1.534
temp (K)	293	150	293	150	273(2)	273(2)
θ range (deg)	3.4–25.2	2.3–25.3	2.1–25.3	2.1–25.3	2.54–22.13	2.57–27.67
measd rflns	5451	5154	2839	5368	14764	10160
indep rflns	4893	4629	2573	5070	3156	5028
<i>R</i> <sub>int</sub>	0.0154	0.0391	0.0286	0.0349	0.0493	0.0214
final <i>R</i> indices	0.0554	0.0385	0.0359	0.0476	0.0484	0.0330
[ <i>I</i> > 2σ( <i>I</i> )]						
<i>R</i> indices (all data)	0.1177	0.1126	0.0979	0.1354	0.1263	0.1065
params	354	354	178	703	159	361

<sup>a</sup> Mo Kα radiation (λ = 0.71073 Å).**Table 2.** Selected and Comparative Metal–Ligand (oxygen) Bond Lengths of Different Complexes

	<b>2</b>	<b>3</b>	<b>4</b>	<b>8<sup>a</sup></b>
Mo(1)–O(1)	1.785(11)	1.744(3)	1.745(3)	2.094(2)
Mo(1)–O(2)	1.805(12)	1.735(2)	1.739(9)	2.403(2)
Mo(1)–O(3)	1.842(7)	1.889(10)	2.153(2)	1.669(2)
Mo(1)–O(4)	1.831(9)	1.933(10)	2.004(2)	1.925(2)
Mo(1)–O(5)	2.146(4)	2.172(2)		1.896(2)
Mo(1)–O(6)	2.010(4)	2.001(2)		1.890(2)
Mo(1)–O(7)	2.157(4)	2.179(2)		1.940(2)
Mo(1)–O(8)	2.007(4)	2.009(2)		

	<b>5</b>		<b>6A</b>	
	molecule 1	molecule 2		
Mo(1)–O(1)	1.699(5)	1.706(5)	Mo(1)–O(3) <sup>b</sup>	1.688(3)
Mo(1)–O(2)	1.707(5)	1.702(6)		
Mo(1)–O(3)	2.203(5)	2.190(6)	Mo(1)–O(1)	2.001(2)
Mo(1)–O(4)	2.005(6)	2.000(7)	Mo(1)–O(2)	2.181(2)
Mo(1)–O(5)	2.188(5)	2.209(6)		
Mo(1)–O(6)	1.993(6)	2.004(7)		

<sup>a</sup> For the origin of the labeled oxygen atom, see Figure 7. <sup>b</sup> This, as well as the other Mo–O distances in this column, is equivalent to the corresponding distances shown at the extreme left row.


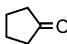
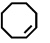
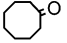
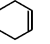
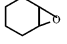
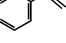
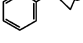
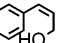
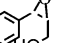
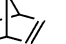
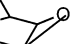
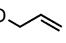
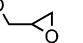
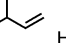

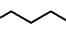
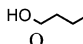
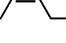
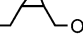
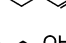
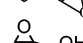
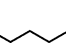
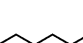
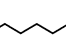
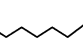
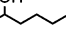
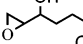
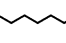
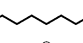
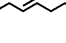
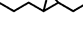
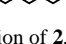
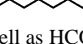
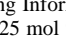
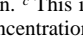
dissolving MoO<sub>3</sub> in H<sub>2</sub>O<sub>2</sub> and treating the resulting solution with the appropriate hydroxamic acids. **5'**, upon recrystallization from dichloromethane (or acetonitrile), converts to **5** (analytical and IR evidence), although, as also described in Experimental Section, compounds **1–4** retain their identity upon recrystallization. However, the conversion of **5'** to **5** could be confirmed only after the crystal structure determination of **5**, since the IR spectrum of **5** and **5'** differ only in contour (relative intensity of ν(Mo=O) and ν(O–O) bands), rather than the position of the bands (for details see section B and Figure 1). The conversion of the labile peroxo complex **5'** (7-coordinate) to **5** (a six coordinate species) during crystallization is because some non-hydrogen atoms of the cinnamoyl group of the ligand (L–L') attain rigidity, being denied the free rotation of C<sub>6</sub>H<sub>5</sub>=C, C=C, and C=O bonds

because the benzenoid π-system is further coupled with the conjugated fragment (viz., –CH=CH–C=O) of the above-mentioned group attached to the metal ion via the carbonyl oxygen, and as a result, the 7-coordinate system becomes sterically strained. To remove the strain, one oxygen atom of the peroxo group is eliminated<sup>44</sup> affording a 6-coordinate dioxo species **5**. This hypothesis is boosted by noting that putative [MoO(O<sub>2</sub>)<sub>2</sub>(BMTHA)]<sup>-</sup> (**7**),<sup>45</sup> expected to be obtained by the incorporation of another peroxo group in **3**, is converted to [MoO(O<sub>2</sub>)<sub>2</sub>(C<sub>6</sub>H<sub>5</sub>COO)] (**8**) because **7** gets sterically strained, and the strain is released via the hydrolysis of BMTHA<sup>-</sup> ligand since, perhaps this process is more facile than the peroxo bond cleavage that occurred in the case of **5** (see later in this section; for confirmation see section C). Complexes **1–4** face no such problem of lability because they are the members of an already known pentagonal bipyramidal family inhabited by a host of oxoperoxo-molybdenum(VI) complexes where the ligand internal bonds have free-rotation character. A reflection of this situation is the molecular structure of **5**, which is shown to contain a mixture of two enantiomers (see section C). Interestingly, an acetonitrile solution of **5** in the presence of H<sub>2</sub>O<sub>2</sub> affords **5'** which, upon recrystallization from acetonitrile, produces **5**. Similar 6-coordinate complexes (viz, **6A–6D**) isolated using A-type ligands, upon structural analysis (**6A**), show very simple structure indicating that the structural interest generated in **5** is caused by the structure difference between the A-type and B-type hydroxamic acids. **6A–6D**, upon

(44) The evolution of 1/2 O<sub>2</sub> may occur via the reaction {MoO(O<sub>2</sub>)<sub>2</sub>}<sup>2+</sup> → {Mo(O<sub>2</sub>)<sub>2</sub>}<sup>2+</sup> + 1/2 O<sub>2</sub> (a). The redox reactions are O<sub>2</sub><sup>2-</sup> + 2e<sup>-</sup> → O<sup>2-</sup> + O<sup>2-</sup> (b), O<sup>2-</sup> → 1/2 O<sub>2</sub> + 2e<sup>-</sup> (c). Adding reactions b and c, we get O<sub>2</sub><sup>2-</sup> + O<sup>2-</sup> → 2O<sup>2-</sup> + 1/2 O<sub>2</sub>.

(45) Complex **7** could not be isolated, but the corresponding complex with BMTHA replaced by QO (8-quinolinolate) could be synthesized using the same recipe, and the QO complex was structurally characterized (see ref 25).

**Table 3.** Details of the Catalytic Epoxidation of Olefinic Compounds

		Olefin $\xrightarrow[3-4 \text{ equiv. H}_2\text{O}_2, 25 \text{ mol\% NaHCO}_3, \text{rt (25}^\circ\text{C), CH}_3\text{CN}]{0.1-0.0067 \text{ mol \%, [MoO(O}_2\text{) (CPHA)}_2\text{)]}$ Epoxide						
Entry	Substrate	Product	Time	%conversion <sup>a</sup>	%Yield <sup>c</sup> GC <sup>b</sup>	%Yield <sup>c</sup> isolated	%Selectivity <sup>d</sup>	TON <sup>e</sup> (TOF) <sup>f</sup>
1			20 min	99	99	—	32	14850(44550) <sup>g</sup>
2			30 min	75	75	69	37	7500 (15000) <sup>g</sup>
3			1h	90	90	—	25	4550 (4550)
4			2.5h	77	76	—	24	3040 (1216)
5			1h	76	74	69	28	1480 (1480)
6			15 min	95	95	90	26	9500 (38000) <sup>g</sup>
7			2.5 h	84	82	—	58	4100 (1640)
8			2 h	86	86	—	44	4300 (2150)
9			1.5 h	99	99	—	36	4950 (3300)
10			1 h	97	97	—	37	4850 (4850)
11			1.5 h	96	96	—	39	4800 (3200)
12			40 min	98	98	91	56	4900 (7350) <sup>g</sup>
13			1 h	95	95	—	52	4750 (4750)
h14			1.5 h	99	99	—	28	4950 (3300)
h15			1.75 h	90	90	—	42	4500 (2570)
h16			1.5 h	94	94	—	24	1880(1243)
h17			1.5 h	98	98	90	26	1960 (1306)
h18			3 h	97	97	90	18	970(323)

<sup>a</sup> A control experiment (omission of **2**, as well as HCO<sub>3</sub><sup>-</sup>) does not show any conversion to epoxide or other probable products. <sup>b</sup> The detailed calculation of GC yield is given as Supporting Information. <sup>c</sup> This is the yield of control experiment, excluding the catalyst **2** only, but not NaHCO<sub>3</sub> which remains in the reaction solution at the same 25 mol % concentration. When the control experiment uses NaHCO<sub>3</sub> at a catalytic concentration, the conversion and yield (%) become negligible. <sup>d</sup> Selectivity is really spectacular in the given time frame. If the stirring is continued for still longer periods, entries 5, 7, 8, and 9 start showing a peak perhaps because of the formation of diols. <sup>e</sup> TON = ratio of moles of product (here epoxide) obtained to the moles of catalyst used. <sup>f</sup> The corresponding TOFs (TON h<sup>-1</sup>) are shown in the parentheses. <sup>g</sup> Values extrapolated. <sup>h</sup> A temperature (30 °C) slightly greater than room temperature is used for these substrates. The mole ratios of the catalyst are as follows: substrate = 1:15 000 (for entry 1), 10 000 (for entries 2 and 6), 5000 (for entries 3–4 and 7–15), 2000 (for entries 5, 16, and 17), and 1000 (for entry 18). For entries 16, 17, and 18, acetonitrile and acetone solvent mixtures were used in 2:1 volume ratio.

moderate H<sub>2</sub>O<sub>2</sub> treatment, produce complexes **1–4**, respectively, and a higher amount of peroxide affords the diperoxo adduct [MoO(O<sub>2</sub>)<sub>2</sub>·2hydroxamic acid], the active catalyst which we could not isolate in this work but its formation as an intermediate product has been assumed by inference.<sup>23</sup> Again, when an excess of H<sub>2</sub>O<sub>2</sub> is used, an anionic diperoxo compound is precipitated when a counteranion (PPh<sub>4</sub><sup>+</sup>) is added as PPh<sub>4</sub>Cl. We expected that the compound should be PPh<sub>4</sub>[MoO(O<sub>2</sub>)<sub>2</sub>(BMTHA)] (**7**), but X-ray structure analysis revealed that it was PPh<sub>4</sub>[MoO(O<sub>2</sub>)<sub>2</sub>(C<sub>6</sub>H<sub>5</sub>COO)] (**8**), which is obviously formed via the hydrolysis of coordinated BMTHA ligand, an inference drawn from the isolation and structural characterization of PPh<sub>4</sub>[MoO(O<sub>2</sub>)<sub>2</sub>(QO)],<sup>25</sup> whose isolation and crystallizability in its turn lies on the compactness of the ligand QO<sup>-</sup> (8-quinolinolate) compared to the

hydroxamate ligand. Hence, all the above discussions predict the course of reaction as depicted in Scheme 3.

In the context of enormous efficiency of our molybdenum catalyst in epoxidation reactions, many other works which were thought to be quite promising at one time have now become mediocre after our current discoveries. However, we should refer the work of Banfi et al.<sup>46</sup> who, using Mn(III) porphyrin catalyst, epoxidized cyclooctene (an easily epoxidizable substrate though) with a TOF of 20 000 h<sup>-1</sup>. Also, an extremely good H<sub>2</sub>O<sub>2</sub> economy was found in the epoxidation of quite a few important substrates by Kamata et al.<sup>47</sup> using  $\gamma$ -silicotungstate catalyst and a high-TON epoxidation of alkenes<sup>48</sup> (albeit requiring a long time (385 h),

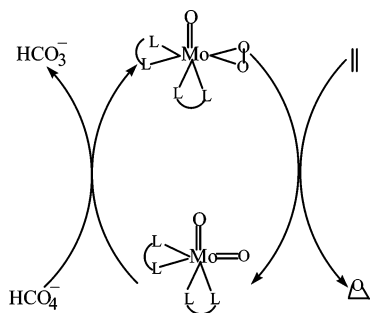
(46) Banfi, S.; Legramandi, F.; Montanari, P.; Possi, G.; Quici, S. *Chem. Commun.* **1991**, 1285–1287.





**Figure 1.** IR spectral contour of the (A)  $\text{MoO}(\text{O}_2)^{2+}$  (**1–4**, **5'**) and (B)  $\text{Mo}(\text{O})_2^{2+}$  (**5**, **6**) moieties.

**Scheme 2.** Stoichiometric (**1–5**) Oxidation of Olefin to Epoxide<sup>a</sup>



<sup>a</sup> L-L = O-O = hydroxamate.

making TOF quite low), using  $\gamma\text{-SiW}_{10}[\text{Fe}^{3+}(\text{OH}_2)_2]\text{O}_{38}^{6-}$  is worth mentioning. However, in the last case, the epoxidation reactions needed a little higher temperature than RT, and so selectivity becomes a bit low.

**B. General Characterization and IR and Electronic spectroscopy.** All the compounds are nonelectrolytes in acetonitrile, and all are diamagnetic. The oxoperoxo metal moieties are characterized by  $\nu(\text{M}=\text{O})$  and  $\nu(\text{O}-\text{O})$  vibrations (see Experimental Section) at a spectral region appropriate for the respective terminal ligands,<sup>49</sup> although the  $\nu(\text{O}-\text{O})$  vibration encroaches toward the  $\nu(\text{M}=\text{O})$  region. The intensity ratio of these vibrations plays a diagnostic role in determining if a particular complex is an oxo-peroxo (strong/medium) or a dioxo (strong/strong) one (compare Experimental Section). Complex **5'** exhibits an s versus m intensity ratio pertaining to the above-mentioned vibrations indicating that the crude complex is an oxo-peroxo complex analogous to **1–4**, and the crystallized version shows both

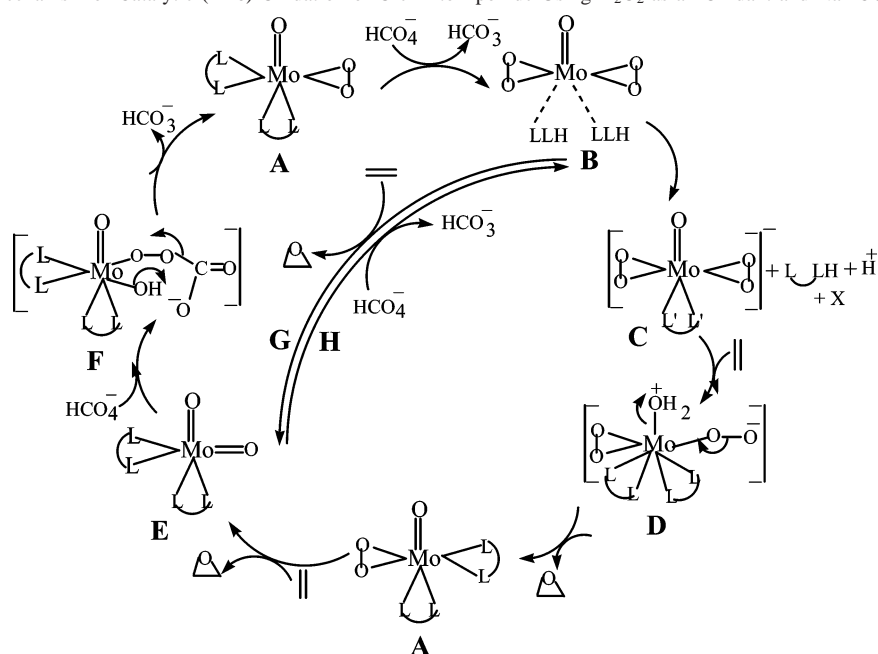
950 and 910  $\text{cm}^{-1}$  bands, having the same intensity (s) as a dioxo complex (**5**). The IR data of both **5** and **5'** are quoted (Experimental Section) showing that we actually isolated **5'** which was converted to **5** during crystallization. This will be more obvious in Figure 1. The 7 coordinate monooxo (peroxo) complexes **1–4** and **5'**, as well as complex **8**, exhibit a single  $\nu(\text{Mo}=\text{O})$  vibration situated at higher than the highest wavenumber region at which the two  $\nu(\text{Mo}=\text{O})$  vibrations appear because of the *cis*-( $\text{MoO}_2$ ) group in 6-coordinate complexes **5** and **6**. This is because the oxo group in the 7-coordinate systems is engaged in forming only one dative  $\text{O } p\pi \rightarrow \text{Mo } d\pi$  overlap, compared to two in dioxo complexes. The  $\nu(\text{C}=\text{O})$  vibrations of uncoordinated BPHAH, BOTHAH, BMTAH, and BPTAH appear at 1640, 1640, 1610, and 1630  $\text{cm}^{-1}$ , respectively. Hence, the downward shift of these vibrations after complexation increases in the following order: **3** < **2** < **1** < **4** (i.e., *m*- < *o*- < *H* < *p*-; see Experimental Section). This indicates that the *m*-tolyl system is most weakly bound to the metal ion via the C=O oxygen. Sterically, it should have been *ortho*, but perhaps a combination of both steric and electronic effect is responsible for this. Interestingly, this order is also corroborated by the appropriate average Mo–O distances (Table 2), as well as the  $\nu(\text{Mo}=\text{O})$  stretching vibration (see Experimental Section). However, the M–O (NO) distance increases in the order **1** (the distance of 2.031 Å<sup>32</sup> seems to be absurd) < **4** < **3** < **2**, which follows the steric hierarchy, but the IR bands in the  $\nu(\text{N}-\text{O})$  region are too weak to be used authentically to examine the parallelism of the IR and X-ray data. The appearance of several vibrations in the low wavenumber region suggests that the asymmetric  $\nu(\text{MoO}_2)$  (triangle),  $\nu(\text{Mo}-\text{O}$  from C=O), and  $\nu(\text{Mo}-\text{O}$  from N–O) occur there, but it is safe not to attempt specific assignment. The IR spectra of B-type ligand, CPHAH, and its metal complexes deserve special attention. Uncoordinated L-L'H shows a sharp and strong band at 1640  $\text{cm}^{-1}$ , which remains unchanged upon coordination. L-L'H also contains two (almost overlapping) stronger (than 1640  $\text{cm}^{-1}$  band) vibrations at 1590 and 1580  $\text{cm}^{-1}$ , indicating that the aliphatic  $\nu(\text{C}=\text{C})$  function is in conjugation with the aromatic ring, as well as with C=O group, giving a picture like {Ph-C=C-}, and it is perhaps quite appropriate to assign the 1640  $\text{cm}^{-1}$  band in CPHAH to the aliphatic  $\nu(\text{C}=\text{C})$  vibration and the latter two bands to the  $\nu(\text{C}=\text{O})$  and  $\nu(\text{C}=\text{C}; \text{aromatic})$  vibrations, respectively. In **5**, the  $\nu(\text{C}=\text{C})$  of the aliphatic and aromatic groups remain unchanged, while the  $\nu(\text{C}=\text{O})$  vibration is red shifted and appears in the 1530  $\text{cm}^{-1}$  region. The position of  $\nu(\text{C}=\text{C})$  (aliphatic) indicates that the aliphatic CH hydrogens are trans with respect to each other.<sup>50</sup> The vibration of the hydroxamate ligands of the complexes **6** are grossly comparable with those of **1–4**. In the case of **8**, the vibrations in this region are distinctly different, and the occurrence of two strong  $\nu(\text{COO}^-)$  bands separated by 80  $\text{cm}^{-1}$  is diagnostic for a chelated  $\text{COO}^-$  group.<sup>49</sup>

(47) Kamata, K.; Yonehara, K.; Sumida, Y.; Yamaguchi, K.; Hikichi, S.; Mizuno, N. *Science* **2003**, *300*, 964–966.

(48) Nishiyama, Y.; Nakagawa, Y.; Mizuno, N. *Angew. Chem., Int. Ed.* **2001**, *40*, 3639–3641.

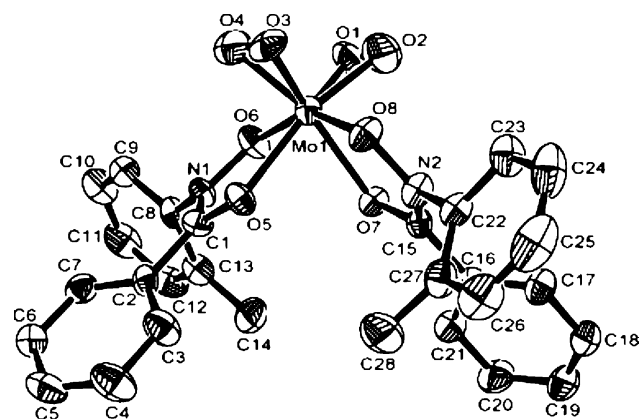
(49) Nakamoto, K. *Infrared and Raman Spectra of Inorganic and Coordination Compounds*, 4th ed.; John Wiley: New York, 1986; p 230.

(50) Avram, M.; Mateescu, G. H. D. *Infrared Spectroscopy*; Wiley-Interscience: Bucharest, Romania, 1972 (copyright by Edutira Technia).

**Scheme 3.** Plausible Mechanism of Catalytic (1–6) Oxidation of Olefin to Epoxide Using  $\text{H}_2\text{O}_2$  as an Oxidant and  $\text{NaHCO}_3$  as Cocatalyst<sup>a</sup>

<sup>a</sup> A was isolated and structurally characterized, since in hydroxamate  $\text{L-L} = \text{O-O}$ . B (drawn by inference) was isolated when  $\text{LL} = 8\text{-quinolinolate}$ ; it was also isolated in the case of  $\text{LL} = \text{hydroxamate}$  when  $\text{M} = \text{W}$  (preliminary unpublished results). C was isolated and structurally characterized, here  $\text{L}'\text{-L}' = \text{benzoate}$  and  $\text{X} = (m\text{-CH}_3)\text{C}_6\text{H}_4\text{NHOH}$  (this hydrolysis does not occur when  $\text{M} = \text{W}$ ). D is an intermediate state. E was isolated and structurally characterized. F is an intermediate state. G is the shunt pathway when  $[\text{H}_2\text{O}_2]$  in the reaction mixture is in moderate excess. H is the shunt pathway when  $[\text{H}_2\text{O}_2]$  in the reaction mixture is in large excess.

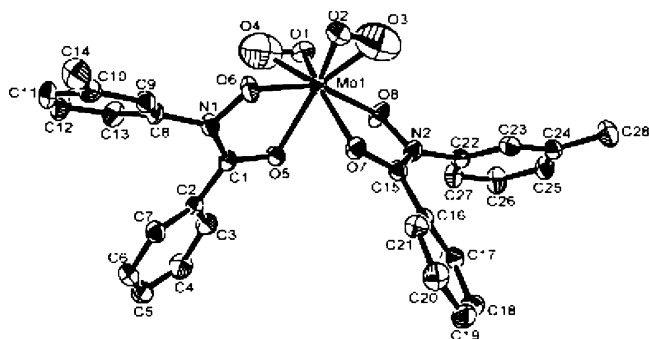
The electronic spectra of the ligands and their metal complexes do not differ *much* in position, profile, and intensity, and so these will not be more informative with respect to their molecular and electronic structure. In uncoordinated hydroxamic acids (viz.,  $\text{L-LH}_1\text{-L-LH}_4$ ), three UV bands appear: one at approximately  $\lambda = 255$  nm for all four ligands ( $\epsilon = 54\,000$ ,  $20\,700$ ,  $18\,500$ , and  $14\,600$   $\text{M}^{-1}\text{cm}^{-1}$ , respectively). The origin of this band is  $\pi \rightarrow \pi^*$  of the aromatic rings. There are two shoulders, one at 270 nm ( $\pi \rightarrow \pi^*$  of  $\text{C}=\text{O}$ ) and another at 330 nm ( $n \rightarrow \pi^*$  of  $\text{C}=\text{O}$  chromophore), respectively. In complexes 1–4, the shoulder at 270 nm remains unchanged, while the band from the  $\pi \rightarrow \pi^*$  transition of the benzene nucleus undergoes a large downward shift showing  $\lambda \approx 230$  nm, which is a natural outcome because of the drainage of electron density from the ring to the  $d^0$  metal ion via the  $\text{C}=\text{O}$  and  $\text{N-O}$  oxygens. Interestingly, the  $n \rightarrow \pi^*$  band of  $\text{C}=\text{O}$  chromophore shows a large upward shift ( $\lambda = 360$  nm) because of the higher energy shift of the nonbonding lone-pair electron of the  $\text{C}=\text{O}$  chromophore. The other lone pair of oxygen, involved in the  $\text{L} \rightarrow \text{M}$   $\sigma$ -overlap, remains unaffected. Gaussian analysis indicate that the intensity of the  $\pi \rightarrow \pi^*$  band is quite high ( $\sim 15\,000$   $\text{M}^{-1}\text{cm}^{-1}$ ) and that of the  $n \rightarrow \pi^*$  one is  $300$   $\text{M}^{-1}\text{cm}^{-1}$ , the molar absorption being in the right direction. Ligand CPHAH, unlike  $\text{L-LH}_1\text{-L-LH}_4$ , shows a prominent absorption at 282 nm occluding the 320 nm band, which however, is revealed on Gaussian analysis. In 5, both the bands are blue shifted. When the spectrum of 5 is recorded by adding 2 drops of  $\text{H}_2\text{O}_2$  in the  $\text{CH}_3\text{CN}$  solution, it becomes comparable with that of 1–4, and this is an important observation indeed, entailing that the lack of bond flexibility of metal–cinnamoyl residue is more a solid-state packing



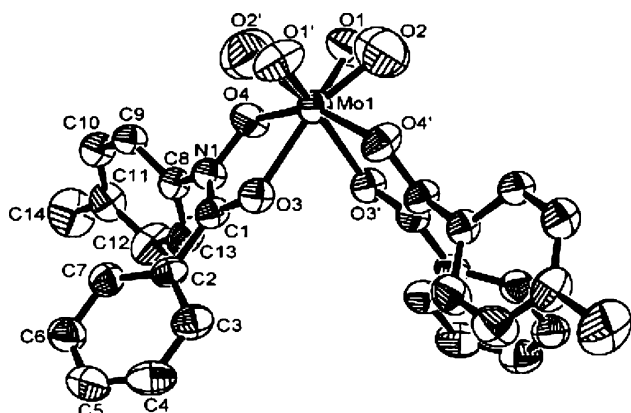
**Figure 2.** Molecular structure of  $[\text{MoO}(\text{O}_2)(\text{BOTHA})_2]$  (2) showing the atom numbering scheme. Thermal ellipsoids are drawn at the 35% probability level. Hydrogen atoms are omitted for clarity. The occupancy factors for the O(1), O(4) atoms are 0.75.

phenomenon than that existing in molecular level in solution. A scrutiny of aliphatic  $\text{C-C}$  and  $\text{C-O}$  bond lengths in the cinnamoyl group of 5 clearly indicates that in the solid-state conjugation<sup>43</sup> certainly exists in the entire cinnamoyl function. The NMR spectral data indicate that 5 also exists as two enantiomeric molecules in solution phase.

**C. Molecular Structure.** The solid-state structures of the three peroxo compounds (viz.,  $[\text{MoO}(\text{O}_2)(\text{BOTHA})_2]$  (2),  $[\text{MoO}(\text{O}_2)(\text{BMTHA})_2]$  (3), and  $[\text{MoO}(\text{O}_2)(\text{BPHTA})_2]$  (4)) are shown in Figures 2–4 respectively, and selected molecular geometric parameters are listed in Tables 1–3 of the Supporting Information; the metal–oxygen distances of all the complexes are listed in Table 2. In all three compounds, the Mo atom is bonded to one oxo and one peroxo group and two bidentate  $\text{BOTHA}^-/\text{BMTHA}^-/\text{BPHTA}^-$  ligands.



**Figure 3.** Molecular structure of  $[\text{MoO}(\text{O}_2)(\text{BMTHA})_2]$  (**3**) showing the atom numbering scheme. Thermal ellipsoids are drawn at the 50% probability level. Hydrogen atoms are omitted for clarity. The occupancy factors for the O(1) and O(2) atoms are 1.0, and those for the O(3) and O(4) atoms are 0.5.



**Figure 4.** Molecular structure of  $[\text{MoO}(\text{O}_2)(\text{BPTHA})_2]$  (**4**) showing the atom numbering scheme. The atoms with prime are generated by the symmetry  $-x, y, 0.5 - z$ . The thermal ellipsoids are drawn at the 35% probability level, and the hydrogen atoms are omitted for clarity.

The oxo and peroxo groups are disordered in all three compounds, and these have been modeled with fractional occupancies to obtain the best refinement results (see Experimental Section). The bond lengths involving these groups ( $\text{Mo}-\text{O}(\text{oxo/peroxo}) = 1.785(11)-1.842(7)$  (**2**),  $1.735(2)-1.933(10)$  (**3**), and  $1.739(1)-1.745(1)$  Å (**4**);  $\text{O}-\text{O}$  (peroxo) =  $0.988(14)-1.150(11)$  (**2**),  $1.149(12)-1.185(10)$  (**3**), and  $1.047(11)$  Å (**4**)) appear to have been affected by the disorder, and these values should be treated with some caution. The overall structural features of the compounds including the dispositions of the oxo and peroxo groups, however, have been established beyond any doubt. In all three structures, the oxo and peroxo groups are mutually cis with angles of  $77.6(5)$  (**2**),  $75.0(4)$  (**3**), and  $83.1(2)^\circ$  (**4**).

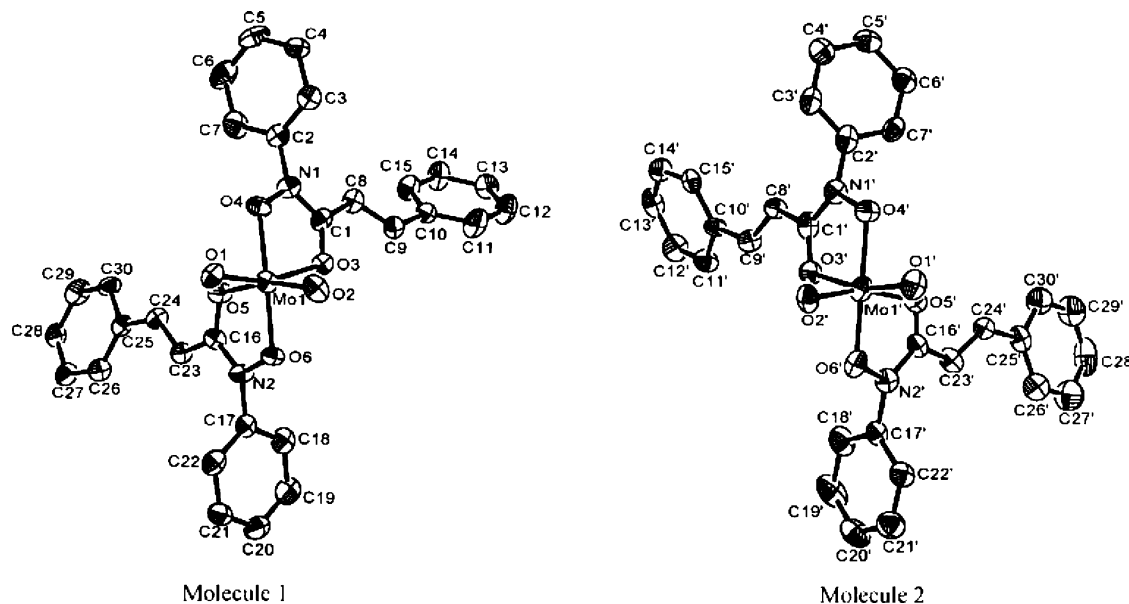
The organic ligands in all three complexes are chelated to the Mo center through the (CO) and (NO) oxygen atoms. The  $\text{Mo}-\text{O}(\text{CO})$  bond distances ( $2.146(4)$ ,  $2.157(4)$  (**2**);  $2.172(2)$ ,  $2.179(2)$  (**3**);  $2.150(2)$  (**4**) Å) and the  $\text{Mo}-\text{O}(\text{NO})$  bond lengths ( $2.010(4)$ ,  $2.007(4)$  (**2**);  $2.001(2)$ ,  $2.009(2)$  (**3**);  $2.004(4)$  (**4**) Å) in the compounds are comparable to the corresponding values related in the reported compounds (e.g.,  $[\text{MoO}(\text{O}_2)(\text{BPHA})_2]$  (**1**)).<sup>32</sup> The observed shortening of the  $\text{Mo}-\text{O}(\text{NO})$  distances (av  $2.006$  Å) compared with the  $\text{Mo}-\text{O}(\text{CO})$  bonds (av  $2.161$  Å) in **2–4** suggests that the hydroxamato oxygens in the compounds are more strongly bonded with the metal ion than the carbonyl oxygens. The

average  $\text{Mo}=\text{O}$  (oxo) and  $\text{Mo}-\text{O}$  (peroxo) distances agree with those observed in analogous oxoperoxo molybdenum compounds ligated with 8-quinolino<sup>23,25</sup> and  $\alpha$ -amino acids.<sup>11a</sup> However, the average  $\text{O}-\text{O}$  (peroxo) distance in the present work is slightly shorter than that of the BPHA compound (**1**) having similar disorder and significantly smaller than that reported for compounds free from any such disorder.<sup>23,50,51</sup>

The bond lengths and bond angles of the coordinated BOTHA, BMTHA, and BPTHA ligands in the three compounds are, as expected, mutually comparable. However, there are significant differences in the relative orientations of the ligands. The five-membered  $\text{MoO}_2\text{CN}$  chelate rings are slightly nonplanar and folded along the  $\text{O}\cdots\text{O}$  axis, as shown by the dihedral angles  $4.4(5)$  and  $5.6(5)^\circ$  (**2**),  $5.2(2)$  and  $12.8(1)^\circ$  (**3**), and  $2.1(3)^\circ$  (**4**) between the  $\text{MoO}_2$  and  $\text{O}_2\text{-CN}$  planes in the chelates. The dihedral angles between the pair of  $\text{MoO}_2$  chelates in the compounds ( $79.2(2)$  (**2**),  $78.9(1)$  (**3**), and  $79.5(2)^\circ$  (**4**)) are nearly the same, but there are significant differences in the orientations of the phenyl rings. Thus the two phenyl rings on each ligand have dihedral angles  $80.1(2)$ ,  $70.2(2)$  (**2**),  $54.5(1)$ ,  $74.4(1)$  (**3**), and  $66.5(1)^\circ$  (**4**) between them. The phenyl ring on the carbon atom of the ligand is rotated out of the corresponding  $\text{O}_2\text{CN}$  plane by  $26.2(3)$  and  $30.2(3)^\circ$  (**2**),  $31.5(1)$  and  $27.5(1)^\circ$  (**3**), and  $25.2(2)^\circ$  (**4**) and that on the nitrogen atom by  $78.8(2)$  and  $67.1(2)^\circ$  (**2**),  $42.7(1)$  and  $60.7(1)^\circ$  (**3**), and  $63.1(1)^\circ$  (**4**). These differences are also reflected in the relevant torsion angles and may be attributed to the inter-ring contacts and the substitution of the methyl group at different positions in the ortho (**2**), meta (**3**) and para (**4**) derivatives.

The crystal structure of **5** consists of discrete molecules of  $[\text{Mo}(\text{O})_2(\text{CPHA})_2]$ , two of which constitute an asymmetric unit. The structure of this molecule is shown in Figure 5, and metal–oxygen bond distances are listed in Table 2. The Mo atoms are octahedral with the chelated organic ligands spanning different edges and producing two “optical isomers”. The two molecules have correct stereochemistry, and they appear to be related by a mirror plane. Since the system is a cis–bis chelate of molybdenum and two different molecules came out on structure analysis, one can very well be  $\Delta$  and the other  $\Lambda$ , but the fact that the long and frozen arm of the CPHA ligand holding the pendant phenyl rings, may have an influence on the ligand (whose donors come from the long and the short arms of the same) assisted nature of packing in the unit cell, which in turn, controls the orientation of the rings; the pendant phenyl rings are actually oriented differently. This is revealed by the torsion angles of  $\text{O3}-\text{C1}-\text{C8}-\text{C9} = -16(1)^\circ$  in molecule 1 and  $= -3(1)^\circ$  in molecule 2. Hence, confidently labeling one molecule as  $\Delta$  and the other  $\Lambda$  becomes difficult. However, the corresponding bond lengths and bond angles in the two molecules are virtually identical but some dihedral angles are significantly different. Unlike the above three compounds, compound **5** is free from any disorder, and the distances and angles involving the dioxo group are accurately determined.

(51) March, J. *Advanced Organic Chemistry: Reactions, Mechanism and Structure*, 4th ed.; John Wiley & Sons: Singapore, 1992; p 30–32 and references therein.

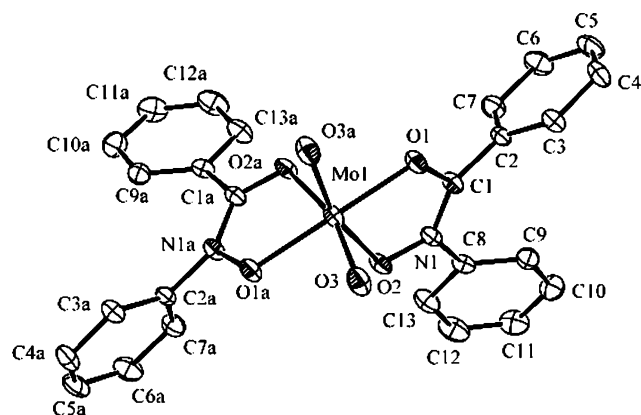


**Figure 5.** Structures of the two independent molecules 1 and 2 of  $[\text{Mo}(\text{O})_2(\text{CPHA})_2]$  (**5**) showing the atom numbering scheme. The thermal ellipsoids are drawn at the 50% probability level, and the hydrogen atoms are omitted for clarity. The occupancy factors for the O(1) and O(2) atoms are 1.0 and 0.5, respectively.

In each molecule, the two oxo groups are mutually cis with Mo–O(oxo) distances lying in a very narrow range (1.699(5)–1.707(5) Å) and O–Mo–O angles of 103.5(3) and 103.4(3)°. Interestingly, the Ph–C(=C) bond length in **5** is significantly shorter than the Ph–C(=O) length in **1–4**, indicating partial double-bond character of the C(24)–C(25) bond in **5** (which should occur in the case of extended conjugation as mentioned in the section A).

The Mo–O(ON) (2.188(5)–2.209(6) Å) and Mo–O(OC) (1.993(6)–2.005(6) Å) bonds are marginally longer, as are the corresponding values in **2** and **4**. The five-membered chelate rings in **5** are slightly nonplanar with fold angles of 1.9(4)–7.9(3)° about the O⋯O axes. The two five-membered chelate rings in **5** are inclined toward each other by 82.4(2)° in molecule 1 and 81.1(2)° in molecule 2. The dihedral angles between the cinnamoyl phenyl ring (C10–C15, C25–C30; C10'–C15', C25'–C30') and the corresponding MoO<sub>2</sub>CN chelate ring are 50.3(3) and 24.3(3)° in molecule 1 and 32.0(3) and 20.2(4)° in molecule 2, indicating a significant difference in the two –CH=CHPh cinnamoyl phenyl ring orientations. The butterfly conformations (which is characteristic of all the complexes **1–4**, **5**, and **6A**)<sup>30</sup> of two CPHA ligands are attained by the rotation of the phenyl rings about the N–C (involved in extended conjugation) bonds; the dihedral angles between C2–C7/C10–C15, C17–C22/C25–C30, C2'–C7'/C10'–C15', and C17'–C22'/C25'–C30' are 82.0(3), 86.0(4), 71.9(3), and 88.9(4)° respectively.

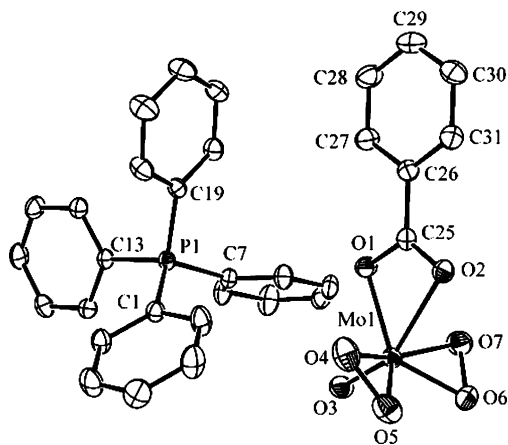
The crystal structure of **6A** is shown in Figure 6, and metal–oxygen bond distances are listed in Table 2. The asymmetric unit in **6A** contains half of the molecule with the Mo atom lying on a 2-fold axis, with the chelated organic ligands spanning different edges. The coordination geometry around the metal center can be described as distorted octahedral with the two oxo groups at a mutually cis position. Unlike compounds **2–4**, compound **6A** is free from any



**Figure 6.** Molecular structure of  $[\text{MoO}_2(\text{BPHA})_2]$  showing the atom numbering scheme.

disorder, and the bond distances and angles involving the dioxo groups in **6A** are determined reliably. The Mo–O(oxo) distances 1.691(2) Å lie within a normal range. The Mo–O(ON) (2.181(2) Å) and Mo–O(OC) (2.001(2) Å) bond lengths are consistent with analogous structure and are nearly the same as the corresponding values in **2–4**. The five-membered chelate rings in **6A** are slightly nonplanar with fold angles of 1.9(4)–7.9(3)° about the O⋯O axes.

The structure of **8** consists of discrete monomeric anions,  $[\text{MoO}(\text{O}_2)_2(\text{C}_6\text{H}_5\text{COO})]^-$ , and  $[\text{PPh}_4]^+$  cations held in the crystal lattice. The geometry around the Mo atom can best be described as distorted pentagonal bipyramidal (Figure 7) with the axial sites being occupied by the O2 and O3 (oxo) ligands. The benzoate oxygen (O1) and peroxo moieties (O4, O5 and O6, O7) define the equatorial plane. This is consistent with the observation that greater stability of the diperoxo molybdate complexes is attained when the two peroxo groups coordinate in the equatorial plane.<sup>26</sup> The Mo–O (oxo) and Mo–O (peroxo) distances (Table 2) are comparable to the corresponding values reported in the literature.<sup>25,26</sup> The lengthening of the Mo–O2 (2.403(2) Å) distance compared



**Figure 7.** Molecular structure of  $[\text{MoO}(\text{O}_2)_2(\text{C}_6\text{H}_5\text{COO})]^-$  with the atom numbering scheme.

to the Mo–O1 (2.094(2) Å) bond length in **8** reflects the strong trans influence of the oxo ligand.

**D. NMR Spectroscopy.** The interesting aspect of a molecular structure involving methyl substituents in compounds **2–4**, as well as the enantiomeric couple (molecule 1 and 2) in compound **5**, is nicely displayed by the  $^1\text{H}$  and  $^{13}\text{C}$  NMR spectra of the compounds **2–5**. The number of  $^{13}\text{C}$  signals from the C=O carbon of compounds **2–4** is 2 for each compound (which matches with the structural discussion in previous paragraph), but interestingly, 4 lines appear for the enantiomeric structures (molecule 1 and 2) exhibited by **5**. Also the number of  $^{13}\text{C}$  signals of the phenyl groups are greater in compound **5** than those present in **2–4**, indicating that the magnetic environments of the carbon atoms of the pendant phenyl groups in the two molecules (1 and 2) are different. Also, the IR suggestion that the  $-\text{CH}=\text{CH}-$  residues in **5** have the protons in the trans position is further confirmed from the  $^1\text{H}$  NMR of **5** which shows that the  $J(\text{H}-\text{H})$  coupling constant here is 15.6 Hz.<sup>52</sup>

**E. Catalytic Properties of the Complexes.** These complexes possess general properties of catalytically oxidizing various olefins to their corresponding epoxides with high selectivity which is shown in the Table 3, where **5'** is used as a representative catalyst. The efficiencies of catalysts **1–4** are very much comparable indicating that electron-repelling methyl substituents have little resultant effect in the catalytic process because the steric versus electronic effect operates in cross purposes, but **5**, which actually is **5'** in the presence of  $\text{H}_2\text{O}_2$ , behaves as a superior catalyst (compare yield and TON). This may be the result of an extended conjugation of the aromatic ring with the planar aliphatic residue (viz.,  $-\text{C}=\text{C}=\text{O}$ ), which implies that the low-lying and delocalized empty antibonding orbital in the catalyst makes the oxidation reactions more facile. The dioxo complexes (**6A–6D**) have lower catalytic efficiencies compared to their oxo-peroxo analogues (**1–4**). On the other hand, the monooxo-diperoxo complex (**8**), regardless of ligand hydrolysis, shows the highest catalytic efficiency among the all isolated complexes, and this is assumed to occur because of the presence of two

**Table 4.** Comparative Catalytic Efficiency of the Catalysts (entries 1–7) in the Oxidation of some Representative Olefins<sup>a</sup>

entry	catalyst	oxidation of cyclohexene ( $t = 1$ h)		oxidation of styrene ( $t = 2.5$ h)	
		yield (%)	TON	yield (%)	TON
1	$[\text{MoO}(\text{O}_2)(\text{BP}(\text{H}_3\text{A})_2)]$ ( <b>1</b> )	80	4000	67	2680
2	$[\text{Mo}(\text{O}_2)(\text{B}(\text{O}(\text{H}_3\text{A}))_2)]$ ( <b>2</b> )	83	4150	70	2800
3	$[\text{MoO}(\text{O}_2)(\text{B}(\text{M}(\text{H}_3\text{A}))_2)]$ ( <b>3</b> )	85	4250	72	2880
4	$[\text{MoO}(\text{O}_2)(\text{B}(\text{P}(\text{H}_3\text{A}))_2)]$ ( <b>4</b> )	82	4100	68	2720
5	$[\text{MoO}(\text{O}_2)(\text{C}(\text{P}(\text{H}_3\text{A}))_2)]$ ( <b>5'</b> )	90	4500	76	3040
6	$[\text{P}(\text{Ph}_4)][\text{MoO}(\text{O}_2)_2(\text{PhCOO})]$ ( <b>8</b> )	93	4650	77	3080
7	$[\text{MoO}_2(\text{B}(\text{M}(\text{H}_3\text{A}))_2)]$ ( <b>6C</b> )	77	3850	66	2640

<sup>a</sup> All the parameters were kept the same as in Table 3.

**Table 5.** Efficiency of the catalyst **5'** using different amount of  $\text{H}_2\text{O}_2$  as oxidant<sup>a</sup>

equiv of $\text{H}_2\text{O}_2$ used (wrt substrate)	oxidation of cyclohexene ( $t = 1$ h)		oxidation of styrene ( $t = 2.5$ h)	
	yield (%) (GC)	TON	yield (%) (GC)	TON
1	63	3150	40	1600
2	78	3900	61	2440
3	90	4500	76	3040
4	94	4700	82	3280
5	96	4800	85	3400

<sup>a</sup> All the parameters were kept the same as in Table 3.

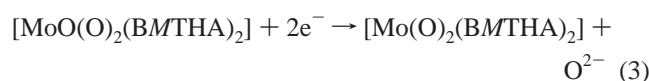
highly reactive peroxo groups. The comparative catalytic activities of the structurally characterized complexes have been studied on two representative olefins shown in Table 4, and on that basis, they can be arranged in order of their increasing activities as **6** (actually here is **6C**) < **1** < **4** < **2** < **3** < **5/5'** < **8**. The efficiency of **5'**, comparable almost to **5**, is caused by the complete facile conversion of the former to the later in the presence of  $\text{H}_2\text{O}_2$ .

To make the method cost-effective,  $\text{H}_2\text{O}_2$  economy is important. Hence, we performed a comparative study on two representative substrates using catalyst **5'** and different molar equivalents of  $\text{H}_2\text{O}_2$  as shown in Table 5. The result shows that the use of 3–4 equiv of  $\text{H}_2\text{O}_2$  is the optimal condition for cost-effectiveness, as well as catalyst efficiency. This is because of the catalase-type decomposition of  $\text{H}_2\text{O}_2$  as a side reaction during the progress of the catalytic oxidation. This  $\text{H}_2\text{O}_2$  loss can be minimized by intermittent addition of  $\text{H}_2\text{O}_2$  rather than addition of the entire amount at once.

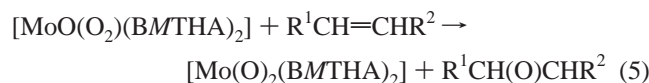
The results obtained using wide varieties of substrates, starting from the highly reactive (to show that TOF may be as high as  $44\ 550\ \text{h}^{-1}$ ) to much less reactive olefins including functionalized olefins (Table 3) clearly indicate the superiority of the present epoxidation method based on the use of high efficiency catalysts. Table 3 also indicates that the speed of reaction, yield, and TOF follow the substrate order carbocyclic > benzylic > lower alkenes > higher alkenes. Moreover, in the cases of aliphatic open-chain olefins, the functionalized (alcoholic) olefins are generally harder to epoxidize than the nonfunctionalized analogues. On the other hand, nonterminal olefins are more easily epoxidized than their terminal analogues. Notably, this method does not epoxidize the conjugated double bond since it did not do so to the C=C group in our catalyst **5**.

(52) Kemp, W. *Organic Spectroscopy*, 3rd ed.; The Macmillan Press Ltd.: Hampshire, U.K., 1991.

**F. Probable Reaction Pathways. F.1. Stoichiometric Reactivity.** We have noted that **6** is incapable of stoichiometrically oxidizing olefins to their epoxides. This is obviously because the oxygen atom from  $\{\text{Mo}(\text{O})_2\}^{2+}$  moiety is not transferable to substrates when the organic ligands used are hydroxamic acids. On the other hand **1–4** and **5'** are capable of furnishing this oxidation by transferring one of the peroxo oxygens to the substrates (see eqs 1–3). Those peroxo compounds can function as a catalyst precursor and, in the presence of  $\text{H}_2\text{O}_2$  and  $\text{NaHCO}_3$ , catalyze the substrate oxidation (Table 3) with a formidable yield (%) and TON. Similarly, **6** also can be regarded as a catalyst precursor generating the catalyst (**1–4** and **5'**) in situ in the presence of a considerable amount of  $\text{H}_2\text{O}_2$ , and then, again it reacts with available  $\text{H}_2\text{O}_2$  if necessary to form the active catalyst. These observations can be represented by the eqs 3–5 and are shown in Scheme 2 with  $\text{BMTHA}^-$  as a representative ligand.



Adding eqs 3 and 4, we get eq 5

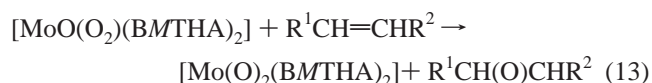
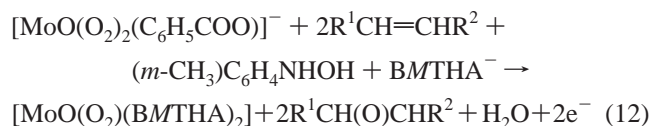
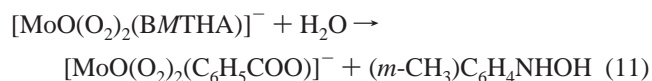
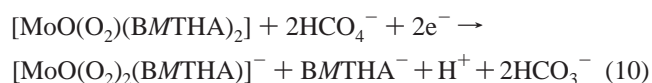
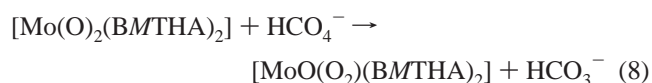


**F.2. Catalytic Reactivity.** Catalytic efficiency when  $\text{H}_2\text{O}_2$  is used as a sole oxidant is rather poor, but when  $\text{NaHCO}_3$  is added as an additive (a cocatalyst), the efficiency of the system becomes enormous. The key aspect<sup>53,54</sup> of such a reaction is that  $\text{H}_2\text{O}_2$  and bicarbonate react in an equilibrium process to produce peroxydicarbonate,  $\text{HCO}_4^-$  (eq 6), which is a more reactive nucleophile than  $\text{H}_2\text{O}_2$  and speeds up the epoxidation reaction. Although  $\text{MoO}(\text{O})_2 \cdot 2\text{BMTHAH}$

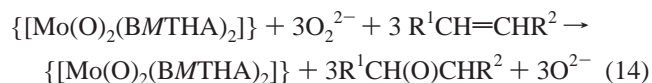


(also true for  $\text{BPHAH}$ ,  $\text{BOTHAH}$ , and  $\text{BPHTAH}$ ) is not isolable in the present case, it was noted earlier<sup>23</sup> that the corresponding product with  $\text{QOH}$  as the ligand (viz.,  $\text{MoO}(\text{O})_2 \cdot 2\text{QOH}$ ) was not only isolated but also was found to have a high formation tendency despite its remarkable reactivity. Attempted crystallization of the  $\text{QOH}$  adduct afforded the less-reactive monoperoxo complex  $[\text{MoO}(\text{O})_2(\text{QO})_2]$ . Moreover, our preliminary work shows that in the oxo-peroxo-tungsten system the corresponding hydroxamic acid adduct,  $\text{WO}(\text{O})_2 \cdot 2\text{BMTHAH}$ , is isolable. So, it may be safely presumed that although the corresponding molybdenum analogue,  $\text{MoO}(\text{O})_2 \cdot 2\text{BMTHAH}$  (**7A**), is not isolable, it may exist in solution and behaves as the active catalyst (**7A**).<sup>23</sup> In that case, the monooxo-monoperoxo complex  $[\text{MoO}(\text{O})_2(\text{hydroxamate})]$  (**1–4** and **5'**) acts as the catalyst

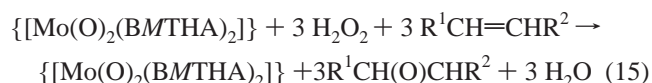
precursor in the presence of a moderate excess of  $\text{H}_2\text{O}_2$ . But in the presence of large excess of  $\text{H}_2\text{O}_2$ , using  $\text{QO}^-$  as the ligand when  $\text{M} = \text{Mo}$  and  $\text{BMTHA}^-$  as the ligand when  $\text{M} = \text{W}$ , the products are  $(\text{PPh}_4)[\text{MoO}(\text{O})_2\text{QO}]$  and  $(\text{PPh}_4)[\text{WO}(\text{O})_2(\text{BMTHA})]$ , respectively. The isolability of the former may be a result of ligand compactness and that of the later a result of the size factor. So, we may infer that the formation of **8** is via the hydrolysis of **7**,  $(\text{PPh}_4)[\text{MoO}(\text{O})_2(\text{BMTHA})]$ , that **7** or **8** is the active catalyst, and that **7A** is the catalyst precursor in the presence of large excess of  $\text{H}_2\text{O}_2$ . Hence, all the above experiments, observations, and logical inferences lead us to frame Scheme 3 to highlight the reaction route of catalytic oxidation of olefins to the respective epoxides in the presence of moderate to large excess, as well as at a condition of nearly spent  $\text{H}_2\text{O}_2$ . Interestingly, as shown in Scheme 3, the original catalyst becomes isolable despite the hydrolysis of the anionic complex, indicating that **8** functions as a surrogate of **7**.



Adding eqs 7–13, we get



that is



It may be emphasized that all the vitally important starting materials are structurally characterized as specified in Scheme 3. Hence, the equations framed and the catalytic cycles drawn have solid foundations.

At this moment, it is very difficult to propose a plausible mechanism of the epoxidation, but the exhibition of very high selectivity precludes any radical mechanism. This was

(53) Yao, H.; Richardson, D. E. *J. Am. Chem. Soc.* **2000**, *122*, 3220–3221.

(54) Lane, B. S.; Vogt, M.; De Rose, V. J.; Burgess, K. *J. Am. Chem. Soc.* **2002**, *124*, 11946–11954.

further corroborated by AIBN (azoisobutyronitrile) and the *p*-benzoquinone test.

It is really a revealing observation that, in the presence of H<sub>2</sub>O<sub>2</sub>, catalyst **5'** is mediocre alone and the cocatalyst at 25 mol % is even more mediocre, but when both the catalyst and cocatalyst are used together, a remarkably higher efficiency is achieved.

**G. Concluding Remarks.** [Mo(O)<sub>2</sub>(Hydroxamate)<sub>2</sub>] (**6**) cannot convert olefins to epoxides stoichiometrically, but in the presence of H<sub>2</sub>O<sub>2</sub> or H<sub>2</sub>O<sub>2</sub> and NaHCO<sub>3</sub>, it can because **6** is converted to [MoO(O<sub>2</sub>)(hydroxamate)<sub>2</sub>] (**6'** ≡ **1–4** and **5'**) which can stoichiometrically effect the olefin → epoxide oxidation. Both classes of compounds (**6** and **6'**) act as efficient catalysts for the oxidation of the described olefins (Table 3) in the presence of NaHCO<sub>3</sub> as the cocatalyst and H<sub>2</sub>O<sub>2</sub> as the terminal oxidant, showing impressive turnover frequencies. In the presence of a considerable excess of H<sub>2</sub>O<sub>2</sub>, the catalytically active species, namely, [MoO(O<sub>2</sub>)<sub>2</sub> (benzoate)]<sup>−</sup> (**8**), is generated (via the hydrolysis of **7**), which performs the oxidation and reverts back to the oxo-peroxo, or the dioxo species, depending on the H<sub>2</sub>O<sub>2</sub> concentration in the reaction medium. Both **6'** and **8** can function as an active catalyst, while **6** behaves as catalyst precursor. If **8** is allowed to be formed, turnover frequency increases. All these are explained in the text; all the classes of compounds (i.e., **1–5**, **6**, and **8**) are structurally characterized, and these compounds can be recovered<sup>55</sup> after the reaction is over and can be used as catalysts in batch 2. After batch 2, which is performed less efficiently than batch 1, the catalysts get almost deactivated. They can, however, be very promptly reactivated using H<sub>2</sub>O<sub>2</sub> and, if necessary, the relevant hydroxamic acids. Successful heterogenization of these homogeneous catalysts should prove very useful from the commercial standpoint.

(55) For **8**, the recovered species are **1–4** depending on the actual catalyst used. This again strongly supports Scheme 3.

Three main products of the reactions suggested for the catalytic cycles are isolated and structurally characterized. The structure of **5**, represented as two enantiomerically related molecular species, is an interesting phenomenon from the structural point of view. Plausible mechanisms for the reaction pathway have been suggested following the chemical principles laid down by current literature.<sup>56,57</sup> Hence the reaction routes and mechanistic outlines should be considered to have solid foundations.

The synthesized complexes used as catalysts in tandem with NaHCO<sub>3</sub> and aqueous H<sub>2</sub>O<sub>2</sub> in CH<sub>3</sub>CN medium at room temperature display high efficiency as determined by yield %, TON, low amount of catalyst loading, better H<sub>2</sub>O<sub>2</sub> economy, very fast conversion rate, high selectivity, experimental simplicity, greenness, and high cost effectiveness which with a little development could be considered almost a real-life process.

**Acknowledgment.** The authors thank the UGC (DSA) and CSIR, New Delhi, for financial assistance. They also thank the Alexander von Humboldt Foundation, Bonn and Amoco Research Center, Naperville, for the donation of the PE 597 IR spectrophotometer and the HP 5880A GC equipment, respectively. The authors also thank DST, New Delhi (Project SR/SI/IC–12/2002), for financing the Agilent 6890 N gas chromatograph used in this work. K.M.A.M. thanks EPSRC for support of the X-ray facilities at Cardiff University. A.K.G. thanks DST-FIST for funding the X-ray diffraction facility at IIT Delhi.

IC0607235

(56) Bruckner, R. *Advanced Organic Chemistry-Reaction Mechanism*; Academic Press: New Delhi, India, 2003.

(57) Sykes P. *A Guide Book to Mechanism in Organic Chemistry*, 6th ed.; Orient Longman Ltd.: New Delhi, India, 1998.